

SKETCHING WITH SPHERICAL DESIGNS FOR NOISY DATA FITTING ON SPHERES*

SHAO-BO LIN[†], DI WANG[‡], AND DING-XUAN ZHOU[§]

Abstract. This paper proposes a sketching strategy based on spherical designs, which is applied to the classical spherical basis function approach for massive spherical data fitting. We conduct theoretical analysis and numerical verifications to demonstrate the feasibility of the proposed sketching strategy. From the theoretical side, we prove that sketching based on spherical designs can reduce the computational burden of the spherical basis function approach without sacrificing its approximation capability. In particular, we provide upper and lower bounds for the proposed sketching strategy to fit noisy data on spheres. From the experimental side, we numerically illustrate the feasibility of the sketching strategy by showing its comparable fitting performance with the spherical basis function approach. These interesting findings show that the proposed sketching strategy is capable of fitting massive and noisy data on spheres.

Key words. Spherical data fitting, spherical basis functions, sketching, spherical designs

AMS subject classifications. 68T05, 94A20, 41A35

1. Introduction. Spherical data abound in our lives: from geophysics [27], quantum chemistry [14], planetary science [51] and astrophysics [26] to computer graphic science [48], image processing [36] and signal recovery [37]. For example, thousands of directional data are collected for image rendering [48]; millions of cosmic microwave background (CMB) observations [26] are gained to analyze the evolution of the Universe; billions of Gravity Recovery and Climate Experiment (GRACE) data [27] are sampled to study gravity and Earth’s natural systems. Different from classical machine learning problems [21] that assume data to be drawn randomly according to some unknown probability distribution, spherical data fitting frequently requires delicate sampling mechanisms to generate deterministic samples.

Sampling according to sampling theorems [37] and quadrature rules [9] are two popular sampling mechanisms to generate spherical data. Since sampling theorems are only valid under some sparseness assumptions, spherical quadrature rules have received considerable attention and can generate most of the existing scattered in the literature [38, 10, 31, 28]. The problem is, however, that the quadrature weights depend heavily on the location of the corresponding quadrature points, resulting in the existence of inactive samples for which the weights are small. Spherical designs are special spherical quadrature rules with equal weights. The equal-weight nature implies

*The corresponding author is Di Wang.

Funding: S. B. Lin was partially supported by the National Key R&D Program of China (No.2020YFA0713900) and the National Natural Science Foundation of China [Grant Nos. 62276209]. D. Wang was partially supported by the National Natural Science Foundation of China [Grant Nos. 61772374]. D. X. Zhou was partially supported in part by the Research Grants Council of Hong Kong [Project Nos. CityU 11308020, N-CityU 102/20, C1013-21GF], Hong Kong Institute for Data Science, Germany/Hong Kong Joint Research Scheme [Project No. G-CityU101/20], Laboratory for AI-Powered Financial Technologies, and National Science Foundation of China [Project No. 12061160462] when he worked at City University of Hong Kong and the first version of the paper was written.

[†]Center for Intelligent Decision-Making and Machine Learning, School of Management, Xi’an Jiaotong University, Xi’an 710049, China (sblin1983@gmail.com).

[‡]Center for Intelligent Decision-Making and Machine Learning, School of Management, Xi’an Jiaotong University, Xi’an 710049, China (wang.di@xjtu.edu.cn).

[§]School of Mathematics and Statistics, University of Sydney, Sydney NSW 2006, Australia (dingxuan.zhou@sydney.edu.au).

the equal-contribution of the quadrature points in spherical designs, which excludes quadrature points associated with small quadrature weights and then reduces the number of sampling points [6]. Due to this, spherical designs have been widely used to construct spherical hyper-interpolations [34] to learn noisy data, produce spherical regularized least squares estimators [1] to fit scattered data, and design non-convex minimization algorithms [12] for signal recovery on spheres.

In this paper, we consider problems of noisy spherical data fitting sampled at spherical t -designs. Let $D := \{(x_i, y_i)\}_{i=1}^{|D|}$ be the set of data with $\{x_i\}_{i=1}^{|D|}$ a spherical t -design and

$$(1.1) \quad y_i = f^*(x_i) + \varepsilon_i, \quad \forall i = 1, \dots, |D|,$$

where $|D|$ denotes the cardinality of D , the noise terms $\{\varepsilon_i\}_{i=1}^{|D|}$ are a set of independent and identical random variables satisfying $E[\varepsilon_i] = 0$ and $|\varepsilon_i| \leq M$ for some $M > 0$, and f^* is a function to model the relation between the input x_i and output y_i . We are interested in developing an effective algorithm to find an approximation of f^* based on the given data D . It should be mentioned that our approach is suitable for applications that the user can determine the sampling mechanism on the sphere since the data inputs are assumed to be spherical designs in (1.1).

If $\varepsilon_i = 0$, $i = 1, \dots, |D|$, finding an approximation of f^* in model (1.1) is the classical interpolation problem, which can be successfully settled by spherical polynomials [53], splines [50] and spherical basis functions (SBF) [42]. In particular, it can be found in [42] that the approximation error of the SBF interpolant can be estimated in terms of the mesh norm, provided f^* is smooth. If $\varepsilon_i \neq 0$, the frequently large condition number of the SBF-based interpolation matrix [40] makes the SBF interpolant sensitive to the noise. In this case, a regularization term is needed to guarantee the well-conditionedness of the interpolation matrix, just as [29, 25] did, the analysis of the fitting performance of the SBF approach with regularization is carried out when the noise is extremely small. Since the kernel matrix of the classical SBF approach is positive definite and usually full, which is different from the sparse matrix generated for Wendland SBF and corresponding multi-level schemes [30], it requires $\mathcal{O}(|D|^2)$ and $\mathcal{O}(|D|^3)$ complexities for storage and computation to solve the corresponding regularized least squares problem for any fixed regularization parameter [25]. These above two phenomena make the SBF approach difficult to apply when the noise is not small and the size of the data is large.

In our previous work [34, 17], we proved that the widely used distributed learning equipped with a divide-and-conquer strategy in machine learning [55] is feasible for noisy and massive spherical data fitting. It should be mentioned that the distributed learning approach proposed in [34, 17] requires multiple computational resources, which may dampen the users' spirits and force them to turn to other scalable and stable fitting algorithms. Our purpose in this paper is to propose a sketching scheme to reduce the computational burden of the SBF approach while maintaining the approximation accuracy. Different from the classical sketching approach in [44, 35] that randomly selects part of columns of the interpolation matrix, we focus on generating another spherical s^* -design with $s^* \leq t$ to be the centers of SBF. We provide both theoretical analysis and numerical verifications for the proposed sketching strategy.

Our contributions can be stated as follows. First, we present upper and lower error estimates for the proposed sketching strategy to show that it succeeds in reducing the computational burden of the SBF approach without sacrificing its fitting accuracy. Second, we present Sobolev-type error estimates for the proposed sketching strategy,

which are different from [25, 17] where the analysis is carried out in the L^2 space. Third, we employ a novel integral operator approach in our proofs, which avoids the well known “native space barrier” [41] that requires f^* to belong to the native space of the SBF. Finally, we conduct two toy simulations to illustrate that the proposed sketching strategy is more suitable than the classical schemes in [44, 35] for noisy data fitting on spheres. All these demonstrate the power of the proposed sketching approach and show its efficiency in fitting massive and noisy spherical data.

The rest of the paper is organized as follows. In the next section, we present a novel sketching strategy based on spherical designs. In Section 3, we analyze the theoretical behaviors of the proposed sketching strategy, whose proofs are postponed to Section 5. In Section 4, we conduct two numerical simulations to verify our assertions.

2. Sketching with Spherical Designs. In this section, after introducing some basic properties of spherical designs, we propose the sketching strategy based on spherical designs.

2.1. Spherical designs. Let \mathbb{S}^d be the unit sphere embedded in the $(d + 1)$ -dimensional Euclidean space \mathbb{R}^{d+1} . For $t \in \mathbb{N}$, denote by Π_t^d the class of all algebraic polynomials of degree at most t defined on \mathbb{S}^d . A spherical t -design, denoted by $\mathcal{T}_t := \{x_i\}_{i=1}^{|\mathcal{T}_t|}$, is a finite subset of \mathbb{S}^d satisfying

$$(2.1) \quad \frac{1}{|\mathcal{T}_t|} \sum_{i=1}^{|\mathcal{T}_t|} \pi(x_i) = \frac{1}{\Omega_d} \int_{\mathbb{S}^d} \pi(x) d\omega(x), \quad \forall \pi \in \Pi_t^d,$$

where $\Omega_d = \frac{2\pi^{\frac{d+1}{2}}}{\Gamma(\frac{d+1}{2})}$ is the volume of \mathbb{S}^d , and $d\omega$ denotes the Lebesgue measure on the sphere. Spherical t -designs were introduced in [15] which also provided a lower bound on the number of points, i.e. $|\mathcal{T}_t| \geq c't^d$ for some $c' > 0$. For a given t , it is meaningless to present an upper bound of $|\mathcal{T}_t|$ since the union of two spherical t -designs is also a spherical t -design. Instead, many studies [54, 3, 6, 7, 8, 52] have been done to establish lower bounds of $|\mathcal{T}_t|$ and find c_0 -tight spherical t -designs defined as follows.

DEFINITION 2.1. *A spherical t -design is said to be c_0 -tight for a positive constant c_0 depending only on d if $|\mathcal{T}_t| = c_0 t^d$.*

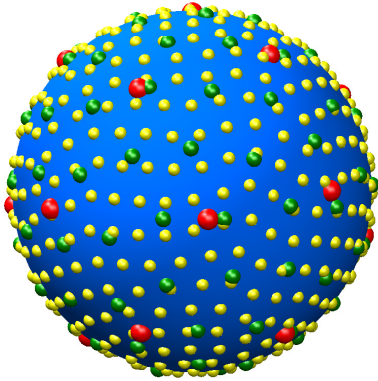
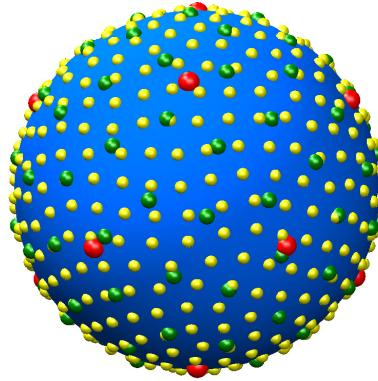
It should be mentioned that the above definition only requires the existence of spherical t -designs with the optimal order of number of points rather than the Delsarte-Goethals-Seidel lower bound ct^d with an absolute constant c [3]. In fact, the Delsarte-Goethals-Seidel lower bound of points of t -designs is known to exist for most t and d . The c_0 -tight spherical t -designs in Definition 2.1 require the achievability of the lower bound $|\mathcal{T}_t| \geq c't^d$ with c' depending on d , which has been verified in the seminal paper [6] as the following lemma.

LEMMA 2.2. *There exists a constant $c_d > 0$, depending only on d , such that for every $N \geq c_d t^d$ and $t \geq 1$, there exists an N -point spherical t -design on \mathbb{S}^d .*

The above lemma demonstrates the existence of c_0 -tight spherical t -designs for any $t \in \mathbb{N}$ and shows that one can design a spherical t -design \mathcal{T}_t satisfying $|\mathcal{T}_t| \sim t^d$. In this way, the classical covering result established in [54] showed that c_0 -tight spherical t -designs have a covering radius (or mesh norm) $h_{\mathcal{T}_t} := \max_{x \in \mathbb{S}^d} \min_{x_i \in \mathcal{T}_t} \arccos(x \cdot x_i) \leq c_1 |\mathcal{T}_t|^{-\frac{1}{d}}$ for some c_1 depending only on d and c_0 , implying that these designs cannot have large holes. However, as the union of two spherical t -designs is a spherical design,

Table 2.1: The number of points for some symmetric spherical t -designs.

Degree t	1	5	9	13	17	21	25	29	33
#points N	2	12	48	94	156	234	328	438	564
Degree t	39	45	51	57	63	69	75	81	87
#points N	782	1038	1328	1656	2018	2418	2852	3324	3830
Degree t	93	99	105	111	117	123	129	135	141
#points N	4374	4952	5568	6218	6906	7628	8388	9182	10014

(a) Spherical t -designs(b) Symmetric spherical t -designsFig. 2.1: Spherical t -designs with $t = 5, 13$, and 29 denoted as red, green, and yellow points, respectively.

c_0 -tight spherical t -designs may have arbitrarily poor separation, i.e., the separation radius $q_{\mathcal{T}_t} := \frac{1}{2} \min_{i \neq i'} \arccos(x_i \cdot x_{i'})$ can be arbitrarily small. The following lemma derived in [7] shows the existence of well separated c_0 -tight spherical t -designs.

LEMMA 2.3. *For $t \in \mathbb{N}$ and $d \geq 2$, there exist c_0 -tight spherical t -designs satisfying $q_{\mathcal{T}_t} \geq c_1 |\mathcal{T}_t|^{-1/d}$, where c_0 and c_1 are constants depending only on d .*

Lemma 2.3 shows that there exist c_0 -tight spherical t -designs whose points are almost evenly distributed on the sphere, i.e., $q_{\mathcal{T}_t} \sim h_{\mathcal{T}_t} \sim |\mathcal{T}_t|^{-1/d}$. Throughout the paper, $a \sim b$ for $a, b \in \mathbb{R}_+$ means that there exists a constant $\hat{c} \geq 1$ depending only on d such that $\hat{c}^{-1}a \leq b \leq \hat{c}a$. Compared with theoretical studies on the existence of c_0 -tight spherical designs, practitioners are also interested in computing lists of spherical t -designs [24, 11, 20, 52], most of which were investigated on \mathbb{S}^2 . In particular, a list of near 1-tight spherical t -designs for $t \leq 21$, $t \leq 100$, and $t \leq 325$ was provided in [24, 11, 52], respectively. We refer interested readers to [8, Sec.2.5] for more information on the constructions of c_0 -tight spherical t -designs. Table 2.1 exhibits the detailed $|\mathcal{T}_t| =: N$ for the spherical t -design developed in [52]. Furthermore, Figure 2.1 presents a geometrical distribution of different spherical t -designs listed in [52] and shows that the constructed spherical t -design is almost equally spaced on \mathbb{S}^2 .

2.2. Sketching with spherical designs. We adopt the widely used SBF approach [25] on data D whose inputs are selected from the c_0 -tight spherical t -

design and outputs satisfying (1.1). Our goal is to develop a novel sketching strategy for fitting massive and noisy spherical data. For $k \in \mathbb{N}$, let P_k^{d+1} be the normalized generalized-Legendre polynomial, i.e., $P_k^{d+1}(1) = 1$ and

$$\int_{-1}^1 P_k^{d+1}(u) P_j^{d+1}(u) (1-u^2)^{\frac{d-2}{2}} du = \frac{\Omega_d}{\Omega_{d-1} Z(d, k)} \delta_{k,j},$$

where $\delta_{k,j}$ is the usual Kronecker symbol and $Z(d, k) \sim k^{d-1}$ denotes the dimension of \mathbb{H}_k^d , the space of spherical harmonics [39] of degree k .

We say that a univariate function $\phi \in L^2[-1, 1]$ is an SBF [41], if its Legendre-expansion $\phi(u) = \sum_{k=0}^{\infty} \hat{\phi}_k \frac{Z(d, k)}{\Omega_d} P_k^{d+1}(u)$ satisfies

$$\hat{\phi}_k := \Omega_{d-1} \int_{-1}^1 P_k^{d+1}(u) \phi(u) (1-u^2)^{\frac{d-2}{2}} du > 0.$$

In addition, if $\sum_{k=0}^{\infty} \hat{\phi}_k \frac{Z(d, k)}{\Omega_d} < \infty$, then ϕ is said to be a positive definite function. It is well known that each SBF ϕ corresponds to a native space

$$\mathcal{N}_\phi := \left\{ f(x) = \sum_{k=0}^{\infty} \sum_{j=1}^{Z(d, k)} \hat{f}_{k,j} Y_{k,j}(x) : \|f\|_\phi^2 := \sum_{k=0}^{\infty} \hat{\phi}_k^{-1} \sum_{j=1}^{Z(d, k)} \hat{f}_{k,j}^2 < \infty \right\},$$

endowed with the inner product $\langle f, g \rangle_\phi := \sum_{k=0}^{\infty} \hat{\phi}_k^{-1} \sum_{j=1}^{Z(d, k)} \hat{f}_{k,j} \hat{g}_{k,j}$, where $\{Y_{k,j}\}_{j=1}^{Z(d, k)}$ is an arbitrary orthonormal basis of \mathbb{H}_k^d and $\hat{f}_{k,j} := \int_{\mathbb{S}^d} f(x) Y_{k,j}(x) d\omega(x)$ is the Fourier coefficient of f . Without loss of generality, we assume

$$(2.2) \quad 0 < \hat{\phi}_k \leq 1, \quad k = 0, 1, \dots$$

throughout the paper. If ϕ is a positive definite function, then \mathcal{N}_ϕ is a reproducing kernel Hilbert space with the reproducing kernel $K(x, x') = \phi(x \cdot x')$.

Regularized least squares based on a positive definite function ϕ is a popular scheme to approximate f^* in the noisy data model (1.1). Given a regularization parameter $\lambda \geq 0$, regularized least squares is defined by

$$(2.3) \quad f_{D, \lambda} = \arg \min_{f \in \mathcal{N}_\phi} \left\{ \frac{1}{|D|} \sum_{i=1}^{|D|} (f(x_i) - y_i)^2 + \lambda \|f\|_\phi^2 \right\}.$$

As an inversion of a $|D| \times |D|$ matrix is involved, the storage and computational complexities for solving (2.3) are $\mathcal{O}(|D|^2)$ and $\mathcal{O}(|D|^3)$, respectively.

For $s^* \leq t$, let $\mathcal{T}_{s^*} = \{x_j^*\}_{j=1}^m$ be a c_0 -tight spherical s^* -design with $m = |\mathcal{T}_{s^*}| = c_0 (s^*)^d$. Define

$$(2.4) \quad \mathcal{H}_{\mathcal{T}_{s^*}, \phi} := \left\{ \sum_{j=1}^m a_j \phi_{x_j^*} : a_j \in \mathbb{R} \right\},$$

where $\phi_x(\cdot) := \phi(x, \cdot)$. Sketching with spherical s^* -design is defined by

$$(2.5) \quad f_{D, s^*, \lambda} := \arg \min_{f \in \mathcal{H}_{\mathcal{T}_{s^*}, \phi}} \frac{1}{|D|} \sum_{i=1}^{|D|} (f(x_i) - y_i)^2 + \lambda \|f\|_\phi^2.$$

Direct computation [44] yields

$$(2.6) \quad f_{D,s^*,\lambda}(\cdot) = \sum_{j=1}^m \alpha_j \phi_{x_j^*}(\cdot),$$

where

$$(2.7) \quad (\alpha_1, \dots, \alpha_m)^T = \left(\mathbb{K}_{|D|,m}^T \mathbb{K}_{|D|,m} + \lambda |D| \mathbb{K}_{m,m} \right)^\dagger \mathbb{K}_{|D|,m}^T y_D,$$

\mathbb{A}^\dagger and \mathbb{A}^T respectively denote the Moore-Penrose pseudo-inverse and transpose of a matrix \mathbb{A} , $(\mathbb{K}_{|D|,m})_{i,j} = \phi(x_i \cdot x_j^*)$, $(\mathbb{K}_{m,m})_{j,j'} = \phi(x_j^* \cdot x_{j'}^*)$, and $y_D = (y_1, \dots, y_{|D|})^T$. Therefore, to solve (2.5), it only requires $\mathcal{O}(|D|m)$ and $\mathcal{O}(|D|m^2)$ complexities in storage and computation, respectively, which significantly reduces the storage and computational complexities for solving the regularized least squares (2.3), especially when m is much less than $|D|$. The aim of this paper is to show that such a reduction in computation does not sacrifice the fitting performance of regularized least squares.

In the classical scattered data fitting community, the separation radius is crucial in reflecting the stability of kernel interpolation [40] while the mesh norm is key in the quality of approximation [42, 41]. Thus, a quasi-uniform point set for which the ratio of mesh norm to separation radius is an absolute constant is preferable for analysis. To finalize this section, we present our reasons why we focus on c_0 -tight spherical t -designs rather than quasi-uniform points on the sphere. On one hand, since there is a regularization parameter λ involved in our algorithm (2.5), it is not necessary to assume the separation radius to be comparable with the mesh norm. In particular, our theoretical analysis only requires the equal-weight quadrature rule and a tight number of quadrature points, which is satisfied by the c_0 -tight spherical t -designs. On the other hand, if the quasi-uniform points set is adopted, then the classical sketching algorithm (2.5) [44, 35] should be modified to accommodate the different-weights quadrature rules [10] to guarantee the theoretically optimal approximation error. It would be interesting to design a similar sketching strategy as (2.5) for quasi-uniform point sets and derive the same optimal approximation error estimate as the derived results for spherical designs in the next section.

3. Theoretical Behaviors. There are totally three SBFs involved in our theoretical analysis. The first one is the positive definite function ϕ , which is used to produce the estimator in (2.5). The second one is $\psi(\cdot) = \sum_{k=0}^{\infty} \hat{\psi}_k \frac{Z(d,k)}{\Omega_d} P_k^{d+1}(\cdot)$ satisfying

$$(3.1) \quad \hat{\psi}_k = \hat{\phi}_k^\beta, \quad 0 \leq \beta \leq 1,$$

and it corresponds to a native space \mathcal{N}_ψ where our analysis is carried out. Due to (2.2), (3.1) yields $\hat{\phi}_k \leq \hat{\psi}_k$ and consequently $\mathcal{N}_\phi \subseteq \mathcal{N}_\psi$. It should be mentioned that $\beta = 0$ in (3.1) implies $\mathcal{N}_\psi = L^2(\mathbb{S}^d)$, while $\beta = 1$ yields $\mathcal{N}_\psi = \mathcal{N}_\phi$. The last one is $\varphi(\cdot) = \sum_{k=0}^{\infty} \hat{\varphi}_k \frac{Z(d,k)}{\Omega_d} P_k^{d+1}(\cdot)$ satisfying

$$(3.2) \quad \hat{\varphi}_k = \hat{\phi}_k^\alpha, \quad \alpha \geq \beta,$$

and it is used to quantify the regularity of f^* in terms of $f^* \in \mathcal{N}_\varphi$.

If $\alpha \geq 1$, then (3.2) together with (2.2) implies $\mathcal{N}_\varphi \subseteq \mathcal{N}_\phi$, showing that f^* is in the native space of \mathcal{N}_ϕ . For $\beta \leq \alpha < 1$, we have $\mathcal{N}_\phi \subset \mathcal{N}_\varphi \subseteq \mathcal{N}_\psi$. We refer to

the former as the in-native-space setting, while the latter as the out-of-native-space setting.

It should be mentioned that the analysis of the fitting performances of SBF interpolation or approximation is different [41] for different settings. In particular, the fitting error for algorithm (2.3) with $\lambda \geq 0$ has been established in [42, 29, 25] for the in-native-space setting. However, for the out-of-native-spacing setting, it usually requires more technical skills to conquer the native-space barrier, just as [41] did via a Bernstein-type inequality for SBF. In this paper, we show that the analysis can be unified by using a recently developed integral operator approach on the sphere [17]. The following theorem presents an upper bound estimate for the sketching strategy (2.5).

THEOREM 3.1. *Let $0 < \delta < 1$, D be the data set satisfying (1.1) with $\{\varepsilon_i\}_{i=1}^{|D|}$ being i.i.d. zero-mean random variables satisfying $|\varepsilon| \leq M$, \mathcal{T}_{s^*} be a c_0 -tight spherical s^* -design, ϕ be a positive definite function, and ψ and φ be SBFs satisfying (3.1) and (3.2) with $0 \leq \beta \leq 1$ and $0 \leq \alpha - \beta \leq 1$. If $\hat{\phi}_k \sim k^{-2\gamma}$ with $\gamma > d/2$, $f^* \in \mathcal{N}_\varphi$, $\lambda \sim |D|^{-\frac{2\gamma}{2\gamma(\alpha-\beta)+d}}$, and*

$$(3.3) \quad c|D|^{\frac{2}{2\gamma(\alpha-\beta)+d}} \leq s^* \leq t,$$

then with confidence $1 - \delta$, there holds

$$(3.4) \quad \|J_{\phi,\psi} f_{D,s^*,\lambda} - f^*\|_\psi \leq C|D|^{-\frac{\gamma(\alpha-\beta)}{2\gamma(\alpha-\beta)+d}} \log \frac{3}{\delta},$$

where $J_{\phi,\psi} : \mathcal{N}_\phi \rightarrow \mathcal{N}_\psi$ is the Canonical inclusion, and c and C are constants independent of $|D|$, t , δ , λ and s^* .

Instead of assuming $f^* \in \mathcal{N}_\phi$ [25, 17], our analysis in Theorem 3.1 is carried out for $f^* \in \mathcal{N}_\varphi$ with $0 \leq \alpha - \beta \leq 1$. Such an analysis avoids the classical native-space barrier [41] via showing the same format of error bounds in (3.4) for all α satisfying $0 \leq \alpha - \beta \leq 1$. In particular, if $\beta = 0$ and $0 < \alpha < 1$, then (3.4) reduces to

$$(3.5) \quad \|J_{\phi,\psi} f_{D,s^*,\lambda} - f^*\|_{L^2(\mathbb{S}^d)} \leq C|D|^{-\frac{\alpha\gamma}{2\alpha\gamma+d}} \log \frac{3}{\delta},$$

showing that the proposed sketching strategy (2.5) is also effective even when $f^* \notin \mathcal{N}_\phi$. If we set $\beta = 1$ and $1 < \alpha \leq 2$, then (3.4) reduces to

$$(3.6) \quad \|f_{D,s^*,\lambda} - f^*\|_\phi \leq C|D|^{-\frac{(\alpha-1)\gamma}{2(\alpha-1)\gamma+d}} \log \frac{3}{\delta},$$

presenting Sobolev-type error estimates for noisy data fitting. Since we only impose $0 \leq \beta \leq 1$ and $0 \leq \alpha - \beta \leq 1$ in our analysis, Theorem 3.1 covers numerous (ψ, φ) -pairs adapting to different error analysis frameworks [42, 32, 29, 41, 23, 22, 25, 56, 19, 34, 2].

If we set $s^* = t$, then the sketching strategy (2.5) becomes the classical regularized least squares (2.3). Theorem 3.1 shows that with confidence $1 - \delta$, there holds

$$(3.7) \quad \|J_{\phi,\psi} f_{D,\lambda} - f^*\|_\psi \leq C|D|^{-\frac{\gamma(\alpha-\beta)}{2\gamma(\alpha-\beta)+d}} \log \frac{3}{\delta}.$$

Compared with [17], the derived error estimate is novel in the sense that we provide a larger range of α and β than $\alpha = 1$ and $\beta = 0$. This is non-trivial since our result is available in the out-of-native-space setting. Noting (3.3) and $m = |\mathcal{T}_{s^*}| = c_0(s^*)^d$, we

have $m \geq c_1 |D|^{\frac{2d}{2\gamma(\alpha-\beta)+d}}$ for $c_1 = c_0 c^d$. This implies that the size of sketching depends on γ , α , and β . If $\alpha - \beta = 1$, then $\gamma > d/2$ naturally yields a computation-reduction of the sketching strategy. In general, γ should satisfy $\gamma > d/(2(\alpha - \beta))$.

Finally, comparing the derived estimate (3.7) with the results in [25] with $\alpha = 1$ and $\beta = 0$, the approximation rate of an order $|D|^{-\frac{\gamma}{2\gamma+d}}$ is worse than $|D|^{-\frac{\gamma}{d}}$. This seems that the computation-reduction is built upon a sacrifice of fitting performance at first glance. In the following theorem, we show that the derived error bounds in Theorem 3.1 cannot be essentially improved.

THEOREM 3.2. *Let \mathcal{M} be the set of zero-mean distributions with uniform bound M , D be the data set satisfying (1.1) with $\{\varepsilon_i\}_{i=1}^{|D|}$ drawn i.i.d. according to a distribution in \mathcal{M} , f_D be an arbitrary function derived from D , ϕ , ψ , and φ be SBFs satisfying (3.1) and (3.2) with $0 \leq \beta \leq 1$ and $\alpha - \beta \geq 0$ and $\hat{\phi}_k \tilde{k}^{-2\gamma}$ with $\gamma > d/2$. Then there exists a $\rho^* \in \mathcal{M}$ and an $f_{bad}^* \in \mathcal{N}_\varphi$ with $\|f_{bad}^*\|_\varphi \leq U$ for some $U > 0$ such that*

$$\mathbf{P}_{\rho^*} \left[\|f_D - f_{bad}^*\|_\psi \geq C_1 |D|^{-\frac{\gamma(\alpha-\beta)}{2\gamma(\alpha-\beta)+d}} \right] \geq \frac{1}{4},$$

where \mathbf{P}_{ρ^*} denotes the probability with respect to the distribution ρ^* , and C_1 is a constant independent of $|D|$, δ and t .

Theorem 3.2 shows that the fitting error derived in (3.4) is optimal in a probability sense. Combining Theorem 3.1 with Theorem 3.2, we obtain that the proposed sketching strategy (2.5) maintains the approximation capability of regularized least squares (2.3) while significantly reducing the computational burden. This makes (2.5) available for massive and noisy data fitting problems on spheres. Furthermore, the reason for the degradation in fitting performance is the large amount of noise in the model (1.1) when compared with [25]. In fact, the magnitude of noise M in (1.1) can be comparable with $\|f^*\|_\varphi$, which is far beyond the scope of [25]. As shown in our proof, the accommodation of large noise leaves a large room for sketching, showing that larger noise admits smaller s^* for sketching with spherical s^* -designs. The restriction of s^* in (3.3) is presented for the worst-case analysis since we do not give any lower bound on the magnitude of noise.

4. Numerical Verifications. In this section, some numerical results are reported to verify our theoretical statements. Three sketching methods are employed for comparisons. The first method chooses the first m samples from the training set for the sketching set (denoted by First). The second method randomly chooses m samples from the training set for the sketching set (denoted by Random). These two methods have been widely used for kernel learning with random samples [44, 35] in Euclidean space and provide baselines for our analysis. The third method uses Womersley's symmetric spherical s^* -designs with $m = (s^*)^2/2 + s^*/2 + O(1)$ points [52] * for sketching set (denoted by s^* -designs).

We start by introducing two testing functions. The first function is the Franke function modified by Renka [43, p. 146],

$$\begin{aligned} f_1(x) &= 0.75 \exp(-(9x^{(1)} - 2)^2/4 - (9x^{(2)} - 2)^2/4 - (9x^{(3)} - 2)^2/4) \\ &\quad + 0.75 \exp(-(9x^{(1)} + 1)^2/49 - (9x^{(2)} + 1)/10 - (9x^{(3)} + 1)/10) \\ &\quad + 0.5 \exp(-(9x^{(1)} - 7)^2/4 - (9x^{(2)} - 3)^2/4 - (9x^{(3)} - 5)^2/4) \\ (4.1) \quad &\quad - 0.2 \exp(-(9x^{(1)} - 4)^2 - (9x^{(2)} - 7)^2 - (9x^{(3)} - 5)^2), \end{aligned}$$

*<https://web.maths.unsw.edu.au/%7Eersw/Sphere/EffSphDes/>

where $x = (x^{(1)}, x^{(2)}, x^{(3)})^T$. The second function is constructed via the well known Wendland function [13]

$$(4.2) \quad \tilde{\psi}(u) = (1 - u)_+^8 (32u^3 + 25u^2 + 8u + 1),$$

where $u_+ = \max\{u, 0\}$, and it is defined by

$$(4.3) \quad f_2(x) = \sum_{i=1}^{20} \tilde{\psi}(\|x - z_i\|_2),$$

where z_i ($i = 1, \dots, 20$) are the center points of the regions of an equal area partitioned by Leopardi's recursive zonal sphere partitioning procedure [31] [†]. It should be noted that f_1 is an extremely smooth spherical function, while f_2 is in the Sobolev space $W^r(\mathbb{S}^d)$ with $r = 4.5$ [34].

In the simulations, the inputs $\{x_i\}_{i=1}^N$ of training samples are generated by Womersley's symmetric spherical 141-designs, which includes 10014 points on the unit sphere. The corresponding outputs $\{y_i\}_{i=1}^N$ are generated by the function f_j ($j = 1, 2$) plus truncated Gaussian noise, i.e., for each point x_i ,

$$(4.4) \quad y_i = f_j(x_i) + \varepsilon_i,$$

where ε_i is the independent truncated Gaussian noise $\mathcal{N}(0, \delta^2)$, i.e., ε_i is initially generated by the Gaussian noise $\mathcal{N}(0, \delta^2)$ and then truncated to $[-10, 10]$. The inputs $\{x'_i\}_{i=1}^{N'}$ of testing samples are $N' = 10000$ generalized spiral points on the unit sphere, and the corresponding outputs $\{y'_i\}_{i=1}^{N'}$ are generated by $y'_i = f_j(x'_i)$. For the approximation of testing function f_1 , we use the positive definite function $\phi_1(x_1, x_2) = \exp(-\frac{\|x_1 - x_2\|_2^2}{2\sigma^2})$ with the regularization parameter λ being chosen from the set $\{\frac{1}{2^q} | \frac{1}{2^q} > 10^{-10}, q = 0, 1, 2, \dots\}$ and the width σ being chosen from 10 values that are drawn in a logarithmic, equally spaced interval $[0.1, 1]$ [‡]. For the approximation of testing function f_2 , the positive definite function is defined as $\phi_2(x_1, x_2) = \tilde{\psi}(\|x_1 - x_2\|_2)$ with the regularization parameter λ being chosen from the set $\{\frac{1}{1.5^q} | \frac{1}{1.5^q} > 10^{-10}, q = 0, 1, 2, \dots\}$. All parameters in the simulations are selected by grid search.

The simulations are done for three purposes. The first one is devoted to investigating the approximation performance of sketching with s^* -designs under different levels of truncated Gaussian noise. The second simulation focuses on comparisons for the three sketching methods with different sampling ratios (SRs). The last one aims at giving an intuitive visualization for the recovery results of sketching with s^* -designs.

Simulation 1: In this simulation, we generate the training samples according to (4.4) for truncated Gaussian noise with standard deviations $\delta \in \{0, 0.001, 0.1, 0.5\}$. For each δ , we record RMSEs of sketching with s^* -designs by varying the number s^* in the set $\{1, 3, 5, \dots, 141\}$. It is notable that the case of $s^* = 141$ is the standard regularized least squares (2.3) with training all samples, and then the corresponding RMSE provides a baseline to assess the performance of sketching with s^* -designs. The results of RMSE on the testing set as a function of the number s^* , which corresponds to the sampling ratio (SR), for different levels of truncated Gaussian noise are shown

[†]<http://eqsp.sourceforge.net>

[‡]For the noise-free training data, i.e., $\delta = 0$, the width σ is chosen from 10 values that are drawn in logarithmic, equally spaced interval $[0.028, 0.28]$.

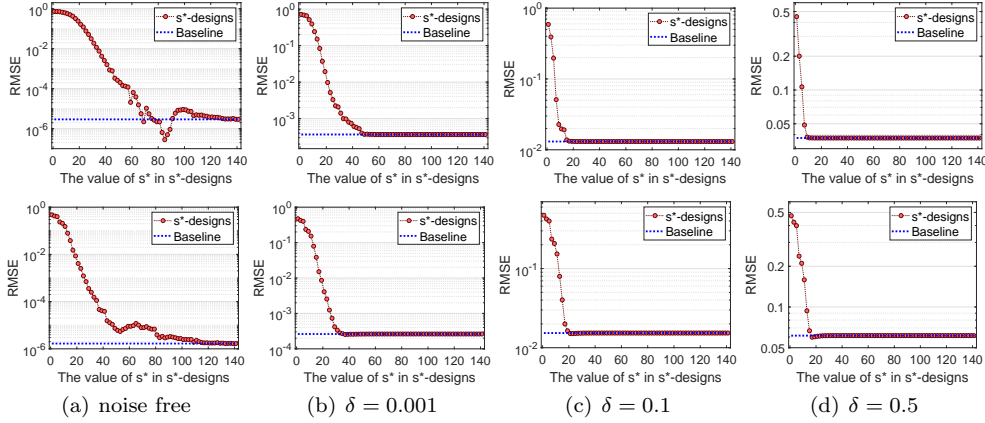


Fig. 4.1: The relation between RMSE and the number s^* for sketching with s^* -designs under different levels of truncated Gaussian noise. The sub-figures of the top and bottom rows are the results for the approximation of f_1 and f_2 , respectively.

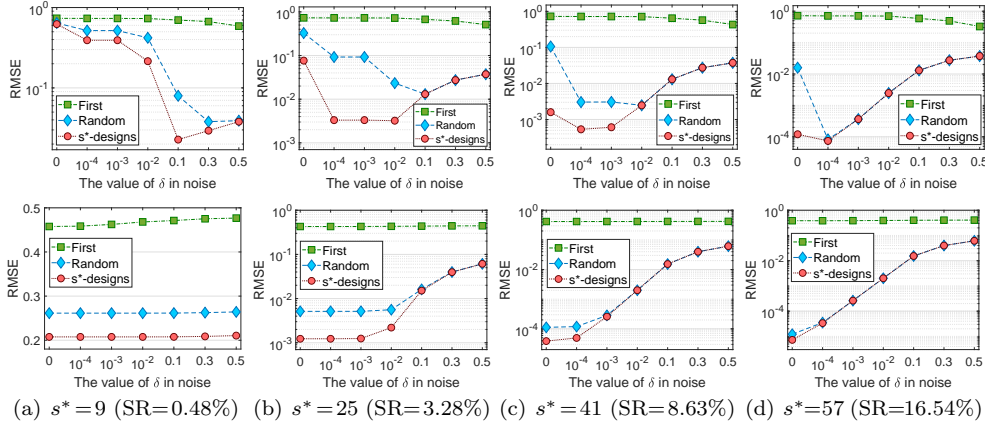


Fig. 4.2: The comparison of RMSE among the three sketching methods with increasing levels of truncated Gaussian noise for fixed numbers of s^* . The sub-figures of the top and bottom rows are the results for the approximation of f_1 and f_2 , respectively.

in Figure 4.1. From the results, we can conclude the following assertions: 1) s^* -designs do not perform very well for noise-free training data ($\delta = 0$), and their accuracy is stable and comparable with regularized least squares only when s^* is larger than 119, i.e., the SR reaches more than 71.32% (the number of samples of 119-designs is 7142, and $\frac{7142}{10014} \approx 0.7132$). 2) For noisy training data, RMSE decreases rapidly as the number s^* increases, reaching the accuracy of regularized least squares under a relatively small s^* . In addition, sketching with s^* -designs is more effective on data with higher levels of truncated Gaussian noise. This verifies our theoretical assertions after Theorem 3.2 that the accommodation of large noise in (1.1) leaves a large room for sketching, implying that larger noise admits smaller s^* for sketching

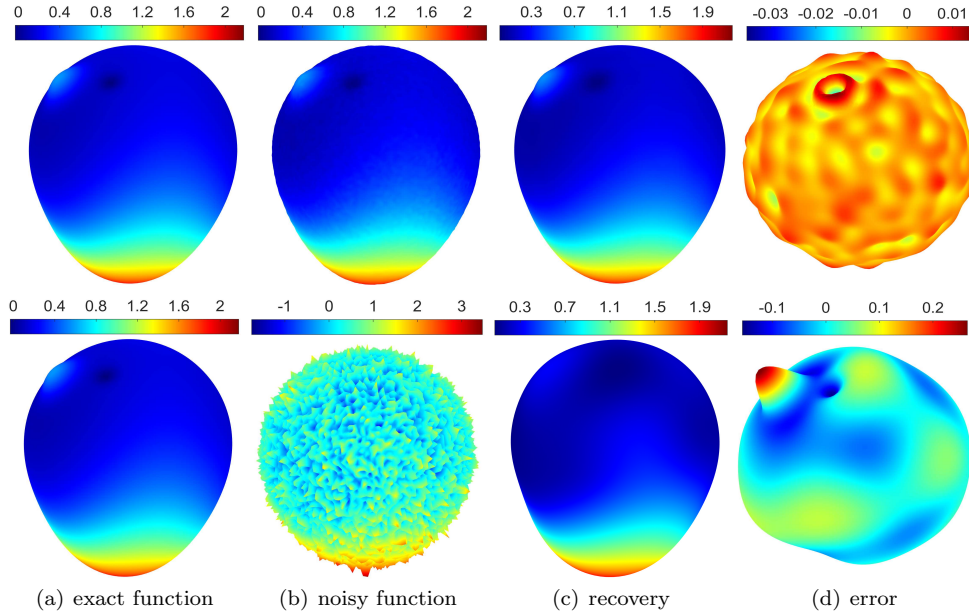


Fig. 4.3: Approximation results of f_1 over the unit sphere (with noise standard deviation $\delta = 0.01$ and $\delta = 0.5$) via sketching with s^* -designs.

with spherical s^* -designs.

Simulation 2: This simulation compares s^* -designs with the other two aforementioned sketching methods by varying standard deviations $\delta \in \{0, 10^{-4}, 10^{-3}, 10^{-2}, 0.1, 0.3, 0.5\}$ of truncated Gaussian noise for fixed numbers $s^* \in \{9, 25, 41, 57\}$. To make a fair comparison, the sizes of sketching sets for the three methods are the same. For example, if we select 25-designs for sketching, i.e., the number of points is 328, then we also select 328 samples from the training set for the other two methods. The relation between RMSE and the standard deviation δ for each fixed number s^* is shown in Figure 4.2. From these results, we have the following observations. 1) Sketching with selecting the first m samples from the training set has the worst performance for all values of δ and s^* . 2) Sketching with randomly selected training samples achieves a noticeable gain in the approximation of the testing functions, because the randomly selected m training samples have more opportunities to construct the overall outline of the testing function than the first m training samples when SR is small. 3) Although the performance of randomly selected training samples is excellent, it can still be significantly improved by using s^* -designs, especially for small SRs. This is the main focus of this paper, which provides a sketching method with a lower SR while maintaining a comparable performance to the standard regularized least squares (2.3).

Simulation 3: In this simulation, some approximation results by using s^* -designs are visualized in Figures 4.3 and 4.4, where the top and bottom rows are the results of the training data with noise standard deviations $\delta = 0.01$ and $\delta = 0.5$, respectively. The sub-figures (a) show the pictures of exact functions, and the sub-figures (b) show the noisy functions (i.e., $f + \varepsilon$). The sub-figures (c) show the

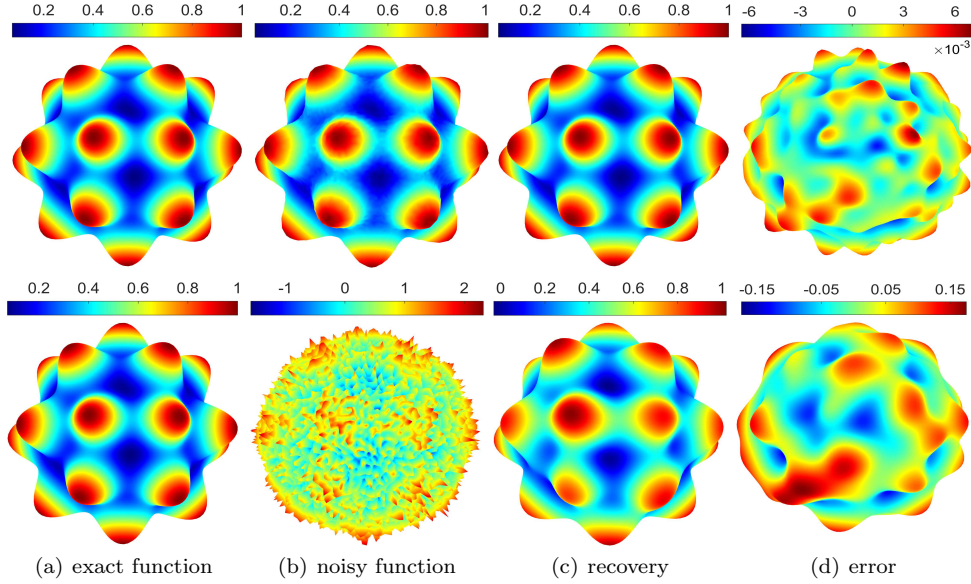


Fig. 4.4: Approximation results of f_2 over the unit sphere (with noise standard deviation $\delta = 0.01$ and $\delta = 0.5$) via sketching with s^* -designs.

approximation of sketching with s^* -designs, where the number $s^* = 33$ in the case of $\delta = 0.01$ and $s^* = 9$ in the case of $\delta = 0.5$ for the function f_1 , and $s^* = 29$ in the case of $\delta = 0.01$ and $s^* = 19$ in the case of $\delta = 0.5$ for the function f_2 . The sub-figures (d) are the visualizations of the corresponding approximation error. These results also verify that sketching with s^* -designs can achieve satisfactory accuracy for the approximation of testing functions when SR is relatively small.

5. Proofs. In this section, we apply the idea of integral operator from [44, 33, 35, 17, 47] and [49, 5, 18] to prove the upper and lower bounds, respectively.

5.1. Preliminaries of positive operators. Before presenting the error analysis, we recall some basic definitions and properties of positive operators established in [4]. Let \mathcal{H}_1 and \mathcal{H}_2 be two Hilbert spaces and $\mathcal{L}(\mathcal{H}_1, \mathcal{H}_2)$ be the space of all bounded linear operators from \mathcal{H}_1 to \mathcal{H}_2 . For $A \in \mathcal{L}(\mathcal{H}_1, \mathcal{H}_2)$, the operator norm is defined by

$$\|A\|_{\mathcal{H}_1 \rightarrow \mathcal{H}_2} = \sup_{\|f\|_{\mathcal{H}_1} \leq 1} \|Af\|_{\mathcal{H}_2}.$$

If $f \in \mathcal{H}_1$, there naturally holds

$$(5.1) \quad \|Af\|_{\mathcal{H}_2} \leq \|A\|_{\mathcal{H}_1 \rightarrow \mathcal{H}_2} \|f\|_{\mathcal{H}_1}.$$

Let A^T be the adjoint operator of A . We have

$$(5.2) \quad \|A\|_{\mathcal{H}_1 \rightarrow \mathcal{H}_2} = \|A^T\|_{\mathcal{H}_2 \rightarrow \mathcal{H}_1} = \|(A^T A)^{1/2}\|_{\mathcal{H}_1 \rightarrow \mathcal{H}_1} = \|A^T A\|_{\mathcal{H}_1 \rightarrow \mathcal{H}_1}^{1/2}.$$

If A is compact, then it can be found in [16, eqs(2.43)] that for any piecewise continuous function $\nu(\cdot) : [0, \infty) \rightarrow [0, \infty)$, there holds

$$(5.3) \quad \nu(AA^T)A = A\nu(A^T A).$$

For $A \in \mathcal{L}(\mathcal{H}, \mathcal{H})$, if $A = A^T$, then A is called self-adjoint. A self-adjoint operator is said to be positive, if $\langle f, Af \rangle_{\mathcal{H}} \geq 0$ for all $f \in \mathcal{H}$. For positive operators A and B , we use the notation $A \preceq B$ to mean that $B - A$ is positive. For $\mu : [0, \infty) \rightarrow [0, \infty)$, define $\mu(A)$ by spectral calculus. We say that μ is operator monotone if

$$A \preceq B \Rightarrow \mu(A) \preceq \mu(B).$$

Operator monotonicity plays an important role in analyzing differences of operators. In particular, the following lemma can be found in [4, Theorem X.1.1].

LEMMA 5.1. *Let $\mu(\cdot)$ be an operator monotone function on $[0, \infty)$ such that $\mu(0) = 0$. Then for any positive operators A and B defined on \mathcal{H} , there holds*

$$\|\mu(A) - \mu(B)\|_{\mathcal{H} \rightarrow \mathcal{H}} \leq \mu(\|A - B\|_{\mathcal{H} \rightarrow \mathcal{H}}).$$

There are numerous operator monotone functions presented in [4, Chapter V], among which the monomial t^r is the most widely used, just as the following lemma [4, Theorem V.1.9] shows.

LEMMA 5.2. *The function $\mu(t) = t^r$ is operator monotone on $[0, \infty)$ for $0 \leq r \leq 1$.*

Based on Lemma 5.1 and Lemma 5.2, we get the following lemma directly.

LEMMA 5.3. *Let $0 \leq r \leq 1$. Then for any positive operators A and B defined on \mathcal{H} , there holds*

$$\|A^r - B^r\|_{\mathcal{H} \rightarrow \mathcal{H}} \leq \|A - B\|_{\mathcal{H} \rightarrow \mathcal{H}}^r.$$

Besides the operator monotonicity, we also need two other lemmas concerning positive operators. The first one is the well known Cordes inequality that can be found in [4, Lemma VII.5.5].

LEMMA 5.4. *Let A and B be positive operators on \mathcal{H} . Then for any $0 \leq r \leq 1$, there holds*

$$\|A^r B^r\|_{\mathcal{H} \rightarrow \mathcal{H}} \leq \|AB\|_{\mathcal{H} \rightarrow \mathcal{H}}^r.$$

The second one, proved in [44, Proposition 6], shows an important property of the projection operator.

LEMMA 5.5. *Let \mathcal{H} , \mathcal{K} , and \mathcal{F} be three separable Hilbert spaces. Let $Z : \mathcal{H} \rightarrow \mathcal{K}$ be a bounded linear operator and P be a projection operator on \mathcal{H} such that $\text{range} P = \text{range} Z^T$. Then for any bounded linear operator $F : \mathcal{F} \rightarrow \mathcal{H}$ and any $\lambda > 0$, we have*

$$\|(I - P)F\|_{\mathcal{F} \rightarrow \mathcal{H}} \leq \lambda^{1/2} \|(Z^T Z + \lambda I)^{-1/2} F\|_{\mathcal{F} \rightarrow \mathcal{H}}.$$

5.2. Operator representation of sketching. Different from the classical approach in [42, 41, 25], our analysis is based on the operator theory presented in the previous subsection. For this purpose, we should at first give an operator representation for (2.5). For any $f \in \mathcal{N}_\phi$, define the sampling operator [45, 46] by $S_D f := (f(x_1), \dots, f(x_{|D|}))^T$, then its scaled adjoint is $S_D^T \mathbf{c} := \frac{1}{|D|} \sum_{i=1}^{|D|} c_i \phi_{x_i}$. Write

$$(5.4) \quad L_{\phi, D} f := S_D^T S_D f = \frac{1}{|D|} \sum_{i=1}^{|D|} f(x_i) \phi_{x_i}, \quad f \in \mathcal{N}_\phi.$$

Then $L_{\phi, D} : \mathcal{N}_\phi \rightarrow \mathcal{N}_\phi$ is a positive operator of rank $|D|$. Throughout the proof, we denote $D_m = \mathcal{T}_{s^*}$ and $\mathcal{H}_{D_m} = \mathcal{H}_{\mathcal{T}_{s^*}, \phi}$ for the sake of brevity. Let P_{D_m} be the projection from \mathcal{N}_ϕ to \mathcal{H}_{D_m} . It is easy to derive that

$$(5.5) \quad (I - P_{D_m})^v = I - P_{D_m}, \quad \forall v \in \mathbb{N}.$$

The following lemma proved in [44, 35] presents an operator representation of $f_{D,s^*,\lambda}$.

LEMMA 5.6. *Let $f_{D,s^*,\lambda}$ be defined by (2.5), then we have*

$$(5.6) \quad f_{D,s^*,\lambda} = g_{D_m,\lambda}(L_{\phi,D})S_D^T y_D,$$

where for a positive operator A ,

$$(5.7) \quad g_{D_m,\lambda}(A) := (P_{D_m}AP_{D_m} + \lambda I)^{-1}P_{D_m}.$$

Since $g_{D_m,\lambda}$ plays a crucial role in our algorithm, we need the following important property of $g_{D_m,\lambda}$ which was proved in [47].

LEMMA 5.7. *Let $g_{D_m,\lambda}$ be defined by (5.7). We have*

$$(5.8) \quad \|(L_{\phi,D} + \lambda I)^{1/2}g_{D_m,\lambda}(L_{\phi,D})(L_{\phi,D} + \lambda I)^{1/2}\|_{\phi \rightarrow \phi} \leq 1,$$

where $\|\cdot\|_{\phi \rightarrow \phi}$ denotes the operator norm from \mathcal{N}_ϕ to \mathcal{N}_ϕ .

We then introduce a data-free limit of $f_{D_m,s^*,\lambda}$. It is easy to derive [35] that the adjoint operator of the Canonical inclusion $J_{\phi,\psi} : \mathcal{N}_\phi \rightarrow \mathcal{N}_\psi$ satisfies

$$J_{\phi,\psi}^T f(x) = \int_{\mathbb{S}^d} \phi(x, x') f(x') d\omega(x'), \quad f \in \mathcal{N}_\psi.$$

Define further $L_{\phi,\psi} = J_{\phi,\psi}J_{\phi,\psi}^T$ and $\mathcal{L}_\phi = J_{\phi,\psi}^T J_{\phi,\psi}$, then $L_{\phi,\psi}$ is an integral operator from $\mathcal{N}_\psi \rightarrow \mathcal{N}_\psi$ and \mathcal{L}_ϕ is an integral operator from $\mathcal{N}_\phi \rightarrow \mathcal{N}_\phi$. In this way, \mathcal{L}_ϕ and $J_{\phi,\psi}^T f^*$ can be regarded as data-free limits of $L_{\phi,D}$ and $S_D^T y_D$, respectively, and therefore

$$(5.9) \quad f_{D_m,\lambda}^\diamond = J_{\phi,\psi} g_{D_m,\lambda}(\mathcal{L}_\phi) J_{\phi,\psi}^T f^*$$

can be regarded as a data-free limit of $J_{\phi,\psi} f_{D,s^*,\lambda}$.

Since $\langle f, \sqrt{\hat{\psi}_k} Y_{k,\ell} \rangle_\psi = \hat{f}_{k,\ell} / \sqrt{\hat{\psi}_k}$, it follows from the well known Funk-Hecke formula [39]

$$(5.10) \quad \int_{\mathbb{S}^d} \phi(x \cdot x') Y_{k,\ell}(x') d\omega(x') = \hat{\phi}_k Y_{k,\ell}(x), \quad \forall \ell = 1, \dots, Z(d, k), \quad k = 0, 1, \dots$$

that for any $f \in \mathcal{N}_\psi$, there holds

$$\begin{aligned} L_{\phi,\psi} f(x) &= \sum_{k=0}^{\infty} \sum_{\ell=1}^{Z(d,k)} \langle f, \sqrt{\hat{\psi}_k} Y_{k,\ell} \rangle_\psi \int_{\mathbb{S}^d} \phi(x \cdot x') \sqrt{\hat{\psi}_k} Y_{k,\ell}(x') d\omega(x') \\ &= \sum_{k=0}^{\infty} \hat{\phi}_k \sum_{\ell=1}^{Z(d,k)} \langle f, \sqrt{\hat{\psi}_k} Y_{k,\ell} \rangle_\psi \sqrt{\hat{\psi}_k} Y_{k,\ell}(x) = \sum_{k=0}^{\infty} \hat{\phi}_k \sum_{\ell=1}^{Z(d,k)} \hat{f}_{k,\ell} Y_{k,\ell}(x). \end{aligned}$$

We then present the following operator representation of $f^* \in \mathcal{N}_\varphi$.

LEMMA 5.8. *If $f^* \in \mathcal{N}_\varphi$, (3.1) and (3.2) hold, then there exists an $h^* \in \mathcal{N}_\psi$ such that*

$$(5.11) \quad f^* = L_{\phi,\psi}^{\frac{\alpha-\beta}{2}} h^*, \quad \text{and} \quad \|f^*\|_\varphi = \|h^*\|_\psi,$$

where $L_{\phi,\psi}^r$ for $r \geq 0$ is defined by spectral calculus, i.e.,

$$L_{\phi,\psi}^r f = \sum_{k=0}^{\infty} \hat{\phi}_k^r \sum_{\ell=1}^{Z(d,k)} \langle f, \sqrt{\hat{\psi}_k} Y_{k,\ell} \rangle_\psi \sqrt{\hat{\psi}_k} Y_{k,\ell}.$$

Proof. Due to (2.2), we can define

$$h^* = \sum_{k=0}^{\infty} \hat{\phi}_k^{\frac{\beta-\alpha}{2}} \sum_{\ell=1}^{Z(d,k)} (\hat{f}^*)_{k,\ell} Y_{k,\ell},$$

then (5.11) obviously holds. The only thing left is to prove $h^* \in \mathcal{N}_\psi$. Due to the definition of $\|\cdot\|_\psi$ and

$$(\hat{h}^*)_{k,\ell} = \int_{\mathbb{S}^d} \sum_{k'=0}^{\infty} \hat{\phi}_{k'}^{\frac{\beta-\alpha}{2}} \sum_{\ell'=1}^{Z(d,k')} (\hat{f}^*)_{k',\ell'} Y_{k',\ell'}(x) Y_{k,\ell}(x) d\omega(x) = \hat{\phi}_k^{\frac{\beta-\alpha}{2}} (\hat{f}^*)_{k,\ell},$$

we have from (3.1) and (3.2) that

$$\begin{aligned} \|h^*\|_\psi^2 &= \sum_{k=0}^{\infty} \hat{\psi}_k^{-1} \sum_{\ell=1}^{Z(d,k)} |(\hat{h}^*)_{k,\ell}|^2 = \sum_{k=0}^{\infty} \hat{\psi}_k^{-1} \sum_{\ell=1}^{Z(d,k)} \hat{\phi}_k^{\beta-\alpha} |(\hat{f}^*)_{k,\ell}|^2 \\ &= \sum_{k=0}^{\infty} \hat{\phi}_k^{-\alpha} \sum_{\ell=1}^{Z(d,k)} |(\hat{f}^*)_{k,\ell}|^2 = \sum_{k=0}^{\infty} \hat{\varphi}_k^{-1} \sum_{\ell=1}^{Z(d,k)} |(\hat{f}^*)_{k,\ell}|^2. \end{aligned}$$

Noting further that $f^* \in \mathcal{N}_\varphi$ implies

$$\|f^*\|_\varphi^2 = \sum_{k=0}^{\infty} \hat{\varphi}_k^{-1} \sum_{\ell=1}^{Z(d,k)} |\hat{f}_{k,\ell}|^2 < \infty,$$

we then have $\|h^*\|_\psi = \|f^*\|_\varphi < \infty$. This completes the proof of Lemma 5.8. \square

5.3. Error decomposition via integral operator. Our analysis is motivated by [35] to divide the fitting error into approximation error, sample error and computational error, respectively.

PROPOSITION 5.9. *Let $f_{D,s^*,\lambda}$ be defined by (2.5). Under (3.1), if $f^* \in \mathcal{N}_\varphi$ with (3.2), then*

$$(5.12) \quad \|J_{\phi,\psi} f_{D,s^*,\lambda} - f^*\|_\psi \leq \mathcal{A}(D, \lambda, m) + \mathcal{S}(D, \lambda, m) + \mathcal{C}(D, \lambda, m),$$

where

$$\begin{aligned} \mathcal{A}(D, \lambda, m) &:= \lambda \|(J_{\phi,\psi} P_{D_m} J_{\phi,\psi}^T + \lambda I)^{-1} (J_{\phi,\psi} P_{D_m} J_{\phi,\psi}^T)^{\frac{\alpha-\beta}{2}} h^*\|_\psi, \\ \mathcal{S}(D, \lambda, m) &:= \mathcal{S}_1(D, \lambda, m) + \mathcal{S}_2(D, \lambda, m) + \mathcal{S}_3(D, \lambda, m), \\ \mathcal{S}_1(D, \lambda, m) &:= \|J_{\phi,\psi} (P_{D_m} L_{\phi,D} P_{D_m} + \lambda I)^{-1} P_{D_m} (J_{\phi,\psi}^T f^* - S_D^T y_D)\|_\psi, \\ \mathcal{S}_2(D, \lambda, m) &:= \|J_{\phi,\psi} (P_{D_m} L_{\phi,D} P_{D_m} + \lambda I)^{-1} P_{D_m} (L_{\phi,D} - \mathcal{L}_\phi) P_{D_m} J_{\phi,\psi}^T \\ &\quad (J_{\phi,\psi} P_{D_m} J_{\phi,\psi}^T + \lambda I)^{-1} (J_{\phi,\psi} P_{D_m} J_{\phi,\psi}^T)^{\frac{\alpha-\beta}{2}} h^*\|_\psi, \\ \mathcal{S}_3(D, \lambda, m) &:= \|J_{\phi,\psi} (P_{D_m} L_{\phi,D} P_{D_m} + \lambda I)^{-1} P_{D_m} (L_{\phi,D} - \mathcal{L}_\phi) P_{D_m} J_{\phi,\psi}^T \\ &\quad (J_{\phi,\psi} P_{D_m} J_{\phi,\psi}^T + \lambda I)^{-1} \left((J_{\phi,\psi} J_{\phi,\psi}^T)^{\frac{\alpha-\beta}{2}} - (J_{\phi,\psi} P_{D_m} J_{\phi,\psi}^T)^{\frac{\alpha-\beta}{2}} \right) h^*\|_\psi, \\ \mathcal{C}(D, \lambda, m) &:= \lambda \|(J_{\phi,\psi} P_{D_m} J_{\phi,\psi}^T + \lambda I)^{-1} \left((J_{\phi,\psi} J_{\phi,\psi}^T)^{\frac{\alpha-\beta}{2}} - (J_{\phi,\psi} P_{D_m} J_{\phi,\psi}^T)^{\frac{\alpha-\beta}{2}} \right) h^*\|_\psi, \end{aligned}$$

and h^* is given in Lemma 5.8.

Proof. Due to the triangle inequality, we get

$$(5.13) \quad \|J_{\phi,\psi} f_{D,s^*,\lambda} - f^*\|_{\psi} \leq \|f_{D_m,\lambda}^{\diamond} - f^*\|_{\psi} + \|f_{D_m,\lambda}^{\diamond} - J_{\phi,\psi} f_{D,s^*,\lambda}\|_{\psi}.$$

It follows from $P_{D_m}^2 = P_{D_m}$ and (5.3) with $A = P_{D_m} J_{\phi,\psi}^T$ that

$$(P_{D_m} J_{\phi,\psi}^T J_{\phi,\psi} P_{D_m} + \lambda I)^{-1} P_{D_m} J_{\phi,\psi}^T = P_{D_m} J_{\phi,\psi}^T (J_{\phi,\psi} P_{D_m} J_{\phi,\psi}^T + \lambda I)^{-1}.$$

Then (5.7) and (5.9) yield

$$\begin{aligned} f_{D_m,\lambda}^{\diamond} - f^* &= (J_{\phi,\psi} g_{D_m,\lambda}(\mathcal{L}_{\phi}) J_{\phi,\psi}^T - I) f^* \\ &= (J_{\phi,\psi} (P_{D_m} J_{\phi,\psi}^T J_{\phi,\psi} P_{D_m} + \lambda I)^{-1} P_{D_m} J_{\phi,\psi}^T - I) f^* \\ &= (J_{\phi,\psi} P_{D_m} J_{\phi,\psi}^T (J_{\phi,\psi} P_{D_m} J_{\phi,\psi}^T + \lambda I)^{-1} - I) f^* \\ &= \lambda (J_{\phi,\psi} P_{D_m} J_{\phi,\psi}^T + \lambda I)^{-1} f^*. \end{aligned}$$

Therefore, it follows from Lemma 5.8 and $L_{\phi,\psi} = J_{\phi,\psi} J_{\phi,\psi}^T$ that

$$(5.14) \quad \begin{aligned} \|f_{D_m,\lambda}^{\diamond} - f^*\|_{\psi} &= \lambda \|(J_{\phi,\psi} P_{D_m} J_{\phi,\psi}^T + \lambda I)^{-1} (J_{\phi,\psi} J_{\phi,\psi}^T)^{\frac{\alpha-\beta}{2}} h^*\|_{\psi} \\ &\leq \lambda \|(J_{\phi,\psi} P_{D_m} J_{\phi,\psi}^T + \lambda I)^{-1} (J_{\phi,\psi} P_{D_m} J_{\phi,\psi}^T)^{\frac{\alpha-\beta}{2}} h^*\|_{\psi} \\ &\quad + \lambda \|(J_{\phi,\psi} P_{D_m} J_{\phi,\psi}^T + \lambda I)^{-1} \left((J_{\phi,\psi} J_{\phi,\psi}^T)^{\frac{\alpha-\beta}{2}} - (J_{\phi,\psi} P_{D_m} J_{\phi,\psi}^T)^{\frac{\alpha-\beta}{2}} \right) h^*\|_{\psi}. \end{aligned}$$

Noting further Lemma 5.6 and (5.9), we obtain

$$\begin{aligned} f_{D_m,\lambda}^{\diamond} - J_{\phi,\psi} f_{D,s^*,\lambda} &= J_{\phi,\psi} \left((g_{D_m,\lambda}(\mathcal{L}_{\phi}) J_{\phi,\psi}^T f^* - (g_{D_m,\lambda}(L_{\phi,D}) S_D^T y_D) \right. \\ &\quad \left. - (P_{D_m} \mathcal{L}_{\phi} P_{D_m} + \lambda I)^{-1} P_{D_m} J_{\phi,\psi}^T f^* - (P_{D_m} L_{\phi,D} P_{D_m} + \lambda I)^{-1} P_{D_m} S_D^T y_D \right). \end{aligned}$$

For positive operators A and B , since $A^{-1} - B^{-1} = B^{-1}(B - A)A^{-1}$, the above estimates yield

$$\begin{aligned} f_{D_m,\lambda}^{\diamond} - J_{\phi,\psi} f_{D,s^*,\lambda} &= J_{\phi,\psi} (P_{D_m} L_{\phi,D} P_{D_m} + \lambda I)^{-1} P_{D_m} (J_{\phi,\psi}^T f^* - S_D^T y_D) \\ &\quad + J_{\phi,\psi} \left((P_{D_m} \mathcal{L}_{\phi} P_{D_m} + \lambda I)^{-1} - (P_{D_m} L_{\phi,D} P_{D_m} + \lambda I)^{-1} \right) P_{D_m} J_{\phi,\psi}^T f^* \\ &= J_{\phi,\psi} (P_{D_m} L_{\phi,D} P_{D_m} + \lambda I)^{-1} P_{D_m} (J_{\phi,\psi}^T f^* - S_D^T y_D) \\ &\quad + J_{\phi,\psi} (P_{D_m} L_{\phi,D} P_{D_m} + \lambda I)^{-1} P_{D_m} (L_{\phi,D} - \mathcal{L}_{\phi}) P_{D_m} (P_{D_m} \mathcal{L}_{\phi} P_{D_m} + \lambda I)^{-1} P_{D_m} J_{\phi,\psi}^T f^*. \end{aligned}$$

Due to Lemma 5.8, the same step as that in (5.14) shows

$$\begin{aligned} &(P_{D_m} \mathcal{L}_{\phi} P_{D_m} + \lambda I)^{-1} P_{D_m} J_{\phi,\psi}^T f^* \\ &= P_{D_m} J_{\phi,\psi}^T (J_{\phi,\psi} P_{D_m} J_{\phi,\psi}^T + \lambda I)^{-1} (J_{\phi,\psi} P_{D_m} J_{\phi,\psi}^T)^{\frac{\alpha-\beta}{2}} h^* \\ &\quad + P_{D_m} J_{\phi,\psi}^T (J_{\phi,\psi} P_{D_m} J_{\phi,\psi}^T + \lambda I)^{-1} \left((J_{\phi,\psi} J_{\phi,\psi}^T)^{\frac{\alpha-\beta}{2}} - (J_{\phi,\psi} P_{D_m} J_{\phi,\psi}^T)^{\frac{\alpha-\beta}{2}} \right) h^*. \end{aligned}$$

Combining the above two equations, we then get

$$\begin{aligned} \|f_{D_m,\lambda}^{\diamond} - J_{\phi,\psi} f_{D,s^*,\lambda}\|_{\psi} &\leq \|J_{\phi,\psi} (P_{D_m} L_{\phi,D} P_{D_m} + \lambda I)^{-1} P_{D_m} (J_{\phi,\psi}^T f^* - S_D^T y_D)\|_{\psi} \\ &\quad + \|J_{\phi,\psi} (P_{D_m} L_{\phi,D} P_{D_m} + \lambda I)^{-1} P_{D_m} (L_{\phi,D} - \mathcal{L}_{\phi}) P_{D_m} J_{\phi,\psi}^T (J_{\phi,\psi} P_{D_m} J_{\phi,\psi}^T + \lambda I)^{-1} \\ &\quad \quad (J_{\phi,\psi} P_{D_m} J_{\phi,\psi}^T)^{\frac{\alpha-\beta}{2}} h^*\|_{\psi} \\ &\quad + \|J_{\phi,\psi} (P_{D_m} L_{\phi,D} P_{D_m} + \lambda I)^{-1} P_{D_m} (L_{\phi,D} - \mathcal{L}_{\phi}) P_{D_m} J_{\phi,\psi}^T (J_{\phi,\psi} P_{D_m} J_{\phi,\psi}^T + \lambda I)^{-1} \\ &\quad \quad \left((J_{\phi,\psi} J_{\phi,\psi}^T)^{\frac{\alpha-\beta}{2}} - (J_{\phi,\psi} P_{D_m} J_{\phi,\psi}^T)^{\frac{\alpha-\beta}{2}} \right) h^*\|_{\psi}. \end{aligned}$$

This together with (5.13) and (5.14) completes the proof of Proposition 5.9. \square

We call $\mathcal{A}(D, \lambda, m)$, $\mathcal{S}(D, \lambda, m)$, and $\mathcal{C}(D, \lambda, m)$ the approximation error, sample error, and computational error, respectively. The sample error reflects the effect of noise and is a quantity to measure the stability of the proposed algorithm; the computational error aims to quantitatively describe the difference between the identity mapping I and projection operator P_{D_m} and, therefore, is mainly devoted to measuring the quality of our sketching strategy; the approximation error focuses on the approximation capability of the sketching algorithm on \mathcal{H}_{D_m} . Based on Proposition 5.9, the estimate of the fitting error can be simplified to bounding $\mathcal{A}(D, \lambda, m)$, $\mathcal{S}(D, \lambda, m)$, and $\mathcal{C}(D, \lambda, m)$, respectively.

5.4. Error estimates via operator differences. The aim of this subsection is to quantify the error via operator (or function) differences. Define

$$(5.15) \quad \mathcal{Q}_{D,\lambda} := \|(\mathcal{L}_\phi + \lambda I)(L_{\phi,D} + \lambda I)^{-1}\|_{\phi \rightarrow \phi},$$

$$(5.16) \quad \mathcal{P}_{D,\lambda} := \|(\mathcal{L}_\phi + \lambda I)^{-1/2}(S_{D_m}^T y_D - L_{\phi,D} f^*)\|_\phi,$$

$$(5.17) \quad \mathcal{R}_{D,\lambda} := \|(\mathcal{L}_\phi + \lambda I)^{-1/2}(L_{\phi,D} - \mathcal{L}_\phi)\|_{\phi \rightarrow \phi}.$$

The following proposition quantifies the fitting error via the above three quantities.

PROPOSITION 5.10. *If $f^* \in \mathcal{N}_\varphi$, and (3.1) and (3.2) hold with $0 \leq \alpha - \beta \leq 1$, then*

$$\|f_{D,s^*,\lambda} - f^*\|_\psi \leq (1 + \mathcal{Q}_{D,\lambda} \mathcal{R}_{D,\lambda} \lambda^{-\frac{1}{2}}) \lambda^{\frac{\alpha-\beta}{2}} (1 + \mathcal{Q}_{\frac{D_m}{2},\lambda}^{\frac{\alpha-\beta}{2}}) \|f^*\|_\varphi + \mathcal{Q}_{D,\lambda} \mathcal{P}_{D,\lambda}.$$

To prove the above proposition, it suffices to bound the corresponding five terms in Proposition 5.9 respectively. For this purpose, we need three auxiliary lemmas.

LEMMA 5.11. *Let F be either a function in \mathcal{N}_ϕ or an operator from \mathcal{N}_ϕ to \mathcal{N}_ϕ , then*

$$\|J_{\phi,\psi}(P_{D_m} L_{\phi,D} P_{D_m} + \lambda I)^{-1} P_{D_m} F\|_* \leq \mathcal{Q}_{D,\lambda} \|(\mathcal{L}_K + \lambda I)^{-1/2} F\|_{**},$$

where $\|F\|_*$ and $\|F\|_{**}$ denote either $\|F\|_\psi$ and $\|F\|_\phi$ respectively if F is a function or $\|F\|_{\phi \rightarrow \psi}$ and $\|F\|_{\phi \rightarrow \phi}$ respectively when F is an operator.

Proof. It follows from (5.1) that

$$\begin{aligned} & \|J_{\phi,\psi}(P_{D_m} L_{\phi,D} P_{D_m} + \lambda I)^{-1} P_{D_m} F\|_* \\ & \leq \|J_{\phi,\psi}(\mathcal{L}_\phi + \lambda I)^{-1/2}\|_{\phi \rightarrow \psi} \|(\mathcal{L}_\phi + \lambda I)^{1/2}(L_{\phi,D} + \lambda I)^{-1/2}\|_{\phi \rightarrow \phi} \\ & \times \|(L_{\phi,D} + \lambda I)^{1/2}(P_{D_m} L_{\phi,D} P_{D_m} + \lambda I)^{-1} P_{D_m} (L_{\phi,D} + \lambda I)^{1/2}\|_{\phi \rightarrow \phi} \\ & \times \|(L_{\phi,D} + \lambda I)^{-1/2}(\mathcal{L}_\phi + \lambda I)^{1/2}\|_{\phi \rightarrow \phi} \|(\mathcal{L}_\phi + \lambda I)^{-1/2} F\|_{**}. \end{aligned}$$

Then, (5.15), Lemma 5.7 and Lemma 5.4 yield

$$\begin{aligned} & \|J_{\phi,\psi}(P_{D_m} L_{\phi,D} P_{D_m} + \lambda I)^{-1} P_{D_m} F\|_* \\ & \leq \|J_{\phi,\psi}(\mathcal{L}_\phi + \lambda I)^{-1/2}\|_{\phi \rightarrow \psi} \mathcal{Q}_{D,\lambda} \|(\mathcal{L}_\phi + \lambda I)^{-1/2} F\|_{**}. \end{aligned}$$

Note further

$$\begin{aligned}
(5.18) \quad & \|J_{\phi,\psi}(\mathcal{L}_\phi + \lambda I)^{-1/2}\|_{\phi \rightarrow \psi}^2 = \sup_{\|f\|_\phi \leq 1} \|J_{\phi,\psi}(\mathcal{L}_\phi + \lambda I)^{-1/2}f\|_\psi^2 \\
& = \sup_{\|f\|_\phi \leq 1} \langle J_{\phi,\psi}(\mathcal{L}_\phi + \lambda I)^{-1/2}f, J_{\phi,\psi}(\mathcal{L}_\phi + \lambda I)^{-1/2}f \rangle_\psi \\
& = \sup_{\|f\|_\phi \leq 1} \langle J_{\phi,\psi}^T J_{\phi,\psi}(\mathcal{L}_\phi + \lambda I)^{-1/2}f, (\mathcal{L}_\phi + \lambda I)^{-1/2}f \rangle_\phi \\
& = \sup_{\|f\|_\phi \leq 1} \|\mathcal{L}_\phi^{1/2}(\mathcal{L}_\phi + \lambda I)^{-1/2}f\|_\phi^2 = \|\mathcal{L}_\phi^{1/2}(\mathcal{L}_\phi + \lambda I)^{-1/2}\|_{\phi \rightarrow \phi}^2 \leq 1.
\end{aligned}$$

We have

$$\|J_{\phi,\psi}(P_{D_m}L_{\phi,D}P_{D_m} + \lambda I)^{-1}P_{D_m}F\|_* \leq \mathcal{Q}_{D,\lambda}\|(\mathcal{L}_K + \lambda I)^{-1/2}F\|_{**}.$$

This completes the proof of Lemma 5.11. \square

LEMMA 5.12. *Let $0 \leq a \leq 1$. For any $0 \leq \alpha - \beta \leq 1$, if $2a \geq \alpha - \beta$, then*

$$\|(J_{\phi,\psi}P_{D_m}J_{\phi,\psi}^T + \lambda I)^{-a}(J_{\phi,\psi}P_{D_m}J_{\phi,\psi}^T)^{\frac{\alpha-\beta}{2}}h^*\|_\psi \leq \lambda^{\frac{\alpha-\beta-2a}{2}}\|h^*\|_\psi.$$

Proof. Since $2a \geq \alpha - \beta$, we have

$$\begin{aligned}
& \|(J_{\phi,\psi}P_{D_m}J_{\phi,\psi}^T + \lambda I)^{-a}(J_{\phi,\psi}P_{D_m}J_{\phi,\psi}^T)^{\frac{\alpha-\beta}{2}}h^*\|_\psi \\
& \leq \|(J_{\phi,\psi}P_{D_m}J_{\phi,\psi}^T + \lambda I)^{-a}(J_{\phi,\psi}P_{D_m}J_{\phi,\psi}^T)^{\frac{\alpha-\beta}{2}}\|_{\psi \rightarrow \psi}\|h^*\|_\psi \\
& \leq \|(J_{\phi,\psi}P_{D_m}J_{\phi,\psi}^T + \lambda I)^{\frac{\alpha-\beta-2a}{2}}\|_{\psi \rightarrow \psi}\|h^*\|_\psi \leq \lambda^{\frac{\alpha-\beta-2a}{2}}\|h^*\|_\psi.
\end{aligned}$$

The proof of Lemma 5.12 is completed. \square

LEMMA 5.13. *Let $0 \leq b \leq 1$. For any $0 \leq \alpha - \beta \leq 1$, there holds*

$$\begin{aligned}
& \|(J_{\phi,\psi}P_{D_m}J_{\phi,\psi}^T + \lambda I)^{-b}((J_{\phi,\psi}J_{\phi,\psi}^T)^{\frac{\alpha-\beta}{2}} - (J_{\phi,\psi}P_{D_m}J_{\phi,\psi}^T)^{\frac{\alpha-\beta}{2}})h^*\|_\psi \\
& \leq \lambda^{\frac{\alpha-\beta-2b}{2}}\mathcal{Q}_{D_m,\lambda}\|h^*\|_\psi.
\end{aligned}$$

Proof. Since $0 \leq \alpha - \beta \leq 1$, we get from Lemma 5.3 that

$$\|(J_{\phi,\psi}J_{\phi,\psi}^T)^{\frac{\alpha-\beta}{2}} - (J_{\phi,\psi}P_{D_m}J_{\phi,\psi}^T)^{\frac{\alpha-\beta}{2}}\|_{\psi \rightarrow \psi} \leq \|J_{\phi,\psi}(I - P_{D_m})J_{\phi,\psi}^T\|_{\psi \rightarrow \psi}^{\frac{\alpha-\beta}{2}}.$$

But (5.5) implies

$$\begin{aligned}
& \|J_{\phi,\psi}(I - P_{D_m})J_{\phi,\psi}^T\|_{\psi \rightarrow \psi} = \|J_{\phi,\psi}(I - P_{D_m})(J_{\phi,\psi}(I - P_{D_m}))^T\|_{\psi \rightarrow \psi} \\
& = \|(I - P_{D_m})J_{\phi,\psi}^T\|_{\psi \rightarrow \phi}^2.
\end{aligned}$$

Then, it follows from (5.18), (5.2), Lemma 5.4 and Lemma 5.5 with $\mathcal{H} = \mathcal{N}_\phi$, $\mathcal{K} = \mathcal{F} = \mathcal{N}_\psi$, and $Z = S_{D_m}$ that

$$\begin{aligned}
& \|(I - P_{D_m})J_{\phi,\psi}^T\|_{\psi \rightarrow \phi} \leq \lambda^{1/2}\|(L_{\phi,D_m} + \lambda I)^{-1/2}J_{\phi,\psi}^T\|_{\psi \rightarrow \phi} \\
& = \lambda^{1/2}\|J_{\phi,\psi}(L_{\phi,D_m} + \lambda I)^{-1/2}\|_{\phi \rightarrow \psi} \leq \lambda^{1/2}\|\mathcal{L}_\phi^{1/2}(L_{\phi,D_m} + \lambda I)^{-1/2}\|_{\phi \rightarrow \phi} \\
& \leq \lambda^{1/2}\mathcal{Q}_{D_m,\lambda}^{1/2}.
\end{aligned}$$

Combining the above three estimates, we get

$$\|(J_{\phi,\psi} J_{\phi,\psi}^T)^{\frac{\alpha-\beta}{2}} - (J_{\phi,\psi} P_{D_m} J_{\phi,\psi}^T)^{\frac{\alpha-\beta}{2}}\|_{\psi \rightarrow \psi} \leq \lambda^{\frac{\alpha-\beta}{2}} \mathcal{Q}_{D_m, \lambda}^{\frac{\alpha-\beta}{2}}.$$

This together with $\|(J_{\phi,\psi} P_{D_m} J_{\phi,\psi}^T + \lambda I)^{-1}\|_{\psi \rightarrow \psi} \leq \lambda^{-b}$ yields

$$\begin{aligned} & \| (J_{\phi,\psi} P_{D_m} J_{\phi,\psi}^T + \lambda I)^{-b} \left((J_{\phi,\psi} J_{\phi,\psi}^T)^{\frac{\alpha-\beta}{2}} - (J_{\phi,\psi} P_{D_m} J_{\phi,\psi}^T)^{\frac{\alpha-\beta}{2}} \right) h^* \|_{\psi} \\ & \leq \| (J_{\phi,\psi} P_{D_m} J_{\phi,\psi}^T + \lambda I)^{-b} \|_{\psi \rightarrow \psi} \| (J_{\phi,\psi} J_{\phi,\psi}^T)^{\frac{\alpha-\beta}{2}} - (J_{\phi,\psi} P_{D_m} J_{\phi,\psi}^T)^{\frac{\alpha-\beta}{2}} \|_{\psi \rightarrow \psi} \| h^* \|_{\psi} \\ & \leq \lambda^{\frac{\alpha-\beta-2b}{2}} \mathcal{Q}_{D_m, \lambda}^{\frac{\alpha-\beta}{2}} \| h^* \|_{\psi}. \end{aligned}$$

The proof of Lemma 5.13 is completed. \square

We are now in a position to prove Proposition 5.10.

Proof of Proposition 5.10. To bound $\mathcal{A}(D, \lambda, m)$, we notice from Lemma 5.12 with $a = 1$ that

$$(5.19) \quad \mathcal{A}(D, \lambda, m) = \lambda \| (J_{\phi,\psi} P_{D_m} J_{\phi,\psi}^T + \lambda I)^{-1} (J_{\phi,\psi} P_{D_m} J_{\phi,\psi}^T)^{\frac{\alpha-\beta}{2}} h^* \|_{\psi} \leq \lambda^{\frac{\alpha-\beta}{2}} \| h^* \|_{\psi}.$$

The definition of $\mathcal{C}(D, \lambda, m)$ and Lemma 5.13 with $b = 1$ yield

$$(5.20) \quad \mathcal{C}(D, \lambda, m) \leq \lambda^{\frac{\alpha-\beta}{2}} \mathcal{Q}_{D_m, \lambda}^{\frac{\alpha-\beta}{2}} \| h^* \|_{\psi}.$$

To bound $\mathcal{S}_1(D, \lambda, m)$, we have from (5.16) and Lemma 5.11 with $F = J_{\phi,\psi}^T f^* - S_{D_m}^T y_D$ that

$$(5.21) \quad \mathcal{S}_1(D, \lambda, m) \leq \mathcal{Q}_{D, \lambda} \mathcal{P}_{D, \lambda}.$$

Noting $P_{D_m}^2 = P_{D_m}$, for an arbitrary $h \in \mathcal{N}_{\psi}$, we obtain

$$(5.22) \quad \begin{aligned} \| P_{D_m} J_{\phi,\psi}^T h \|_{\psi}^2 &= \langle P_{D_m} J_{\phi,\psi}^T h, P_{D_m} J_{\phi,\psi}^T h \rangle_{\phi} = \langle J_{\phi,\psi} P_{D_m} J_{\phi,\psi}^T h, P_{D_m} J_{\phi,\psi}^T h \rangle_{\psi} \\ &= \| J_{\phi,\psi} P_{D_m} J_{\phi,\psi}^T h \|_{\psi}^2 \leq \| (J_{\phi,\psi} P_{D_m} J_{\phi,\psi}^T + \lambda I)^{1/2} h \|_{\psi}^2. \end{aligned}$$

Then, it follows from the definition of $\mathcal{S}_2(D, \lambda, m)$, (5.17), Lemma 5.11 with $F = L_{\phi, D} - \mathcal{L}_{\phi}$, and Lemma 5.12 with $a = 1/2$ that

$$(5.23) \quad \begin{aligned} \mathcal{S}_2(D, \lambda, m) &\leq \| J_{\phi,\psi} (P_{D_m} L_{\phi, D} P_{D_m} + \lambda I)^{-1} P_{D_m} (L_{\phi, D} - \mathcal{L}_{\phi}) \|_{\phi \rightarrow \psi} \\ &\quad \times \| P_{D_m} J_{\phi,\psi}^T (J_{\phi,\psi} P_{D_m} J_{\phi,\psi}^T + \lambda I)^{-1} (J_{\phi,\psi} P_{D_m} J_{\phi,\psi}^T)^{\frac{\alpha-\beta}{2}} h^* \|_{\psi} \\ &\leq \mathcal{Q}_{D, \lambda} \mathcal{R}_{D, \lambda} \| (J_{\phi,\psi} P_{D_m} J_{\phi,\psi}^T + \lambda I)^{-1/2} (J_{\phi,\psi} P_{D_m} J_{\phi,\psi}^T)^{\frac{\alpha-\beta}{2}} \|_{\phi \rightarrow \phi} \| h^* \|_{\psi} \\ &\leq \mathcal{Q}_{D, \lambda} \mathcal{R}_{D, \lambda} \| h^* \|_{\psi} \lambda^{\frac{\alpha-\beta-1}{2}}. \end{aligned}$$

To derive an upper bound of $\mathcal{S}_3(D, \lambda, m)$, we have from Lemma 5.11 with $F = L_{\phi, D} - \mathcal{L}_{\phi}$, Lemma 5.13 with $b = 1/2$, (5.22), and (5.17) that

$$(5.24) \quad \begin{aligned} \mathcal{S}_3(D, \lambda, m) &\leq \| J_{\phi,\psi} (P_{D_m} L_{\phi, D} P_{D_m} + \lambda I)^{-1} P_{D_m} (L_{\phi, D} - \mathcal{L}_{\phi}) \|_{\phi \rightarrow \psi} \\ &\quad \times \| (J_{\phi,\psi} P_{D_m} J_{\phi,\psi}^T + \lambda I)^{-1/2} \left((J_{\phi,\psi} J_{\phi,\psi}^T)^{\frac{\alpha-\beta}{2}} - (J_{\phi,\psi} P_{D_m} J_{\phi,\psi}^T)^{\frac{\alpha-\beta}{2}} \right) h^* \|_{\psi} \\ &\leq \mathcal{Q}_{D, \lambda} \mathcal{R}_{D, \lambda} \lambda^{\frac{\alpha-\beta-1}{2}} \mathcal{Q}_{D_m, \lambda}^{\frac{\alpha-\beta}{2}} \| h^* \|_{\psi}. \end{aligned}$$

Plugging (5.19), (5.20), (5.21), (5.23), and (5.24) into (5.12), we obtain from $\| h^* \|_{\psi} = \| f^* \|_{\varphi}$ that

$$\| f_{D, s^*, \lambda} - f^* \|_{\psi} \leq (1 + \mathcal{Q}_{D, \lambda} \mathcal{R}_{D, \lambda} \lambda^{-\frac{1}{2}}) \lambda^{\frac{\alpha-\beta}{2}} (1 + \mathcal{Q}_{D_m, \lambda}^{\frac{\alpha-\beta}{2}}) \| f^* \|_{\varphi} + \mathcal{Q}_{D, \lambda} \mathcal{P}_{D, \lambda}.$$

This completes the proof of Proposition 5.10. \square

5.5. Proof of Theorem 3.1. Due to Proposition 5.10, it suffices to bound $\mathcal{Q}_{D,\lambda}$, $\mathcal{P}_{D,\lambda}$, and $\mathcal{Q}_{D,\lambda}^*$, which were derived in our recent paper [17].

LEMMA 5.14. *Let $0 < \delta < 1$, $0 \leq v < (2\gamma - d)/2\gamma$, and D satisfy (1.1). If \mathcal{T}_t and $D_m = \mathcal{T}_{s^*}$ are spherical designs and $\hat{\phi}_k \sim k^{-2\gamma}$ with $\gamma > d/2$, then*

$$(5.25) \quad \mathcal{P}_{D,\lambda} \leq \tilde{c}' \lambda^{-\frac{d}{4\gamma}} |D|^{-1/2} \log \frac{3}{\delta},$$

$$(5.26) \quad \mathcal{R}_{D,\lambda} \leq \tilde{c} \lambda^{-1/2} t^{-\gamma},$$

$$(5.27) \quad \mathcal{Q}_{D,\lambda} \leq \begin{cases} \tilde{c}^2 \lambda^{-2+2v} t^{-2(1-v)\gamma} + \tilde{c} \lambda^{-1+v} t^{-(1-v)\gamma} + 1, & \text{if } v \leq 1/2, \\ \tilde{c}^2 \lambda^{-2} t^{-2\gamma} + \tilde{c} \lambda^{-1+v} t^{-(1-v)\gamma} + 1, & \text{if } v > 1/2, \end{cases}$$

$$(5.28) \quad \mathcal{Q}_{D_m,\lambda} \leq \begin{cases} \tilde{c}^2 \lambda^{-2+2v} (s^*)^{-2(1-v)\gamma} + \tilde{c} \lambda^{-1+v} (s^*)^{-(1-v)\gamma} + 1, & \text{if } v \leq 1/2, \\ \tilde{c}^2 \lambda^{-2} (s^*)^{-2\gamma} + \tilde{c} \lambda^{-1+v} (s^*)^{-(1-v)\gamma} + 1, & \text{if } v > 1/2, \end{cases}$$

where \tilde{c} and \tilde{c}' are constants depending only on d and M .

We then prove Theorem 3.1 via using Lemma 5.14 and Proposition 5.10.

Proof of Theorem 3.1. According to (5.27) and (5.26) with $v = 0$, we have from $t \geq s^* \geq \lambda^{-1/\gamma}$ that

$$\mathcal{Q}_{D,\lambda} \mathcal{R}_{D,\lambda} \lambda^{-\frac{1}{2}} \leq \tilde{c}(\tilde{c}^2 + \tilde{c} + 1).$$

Moreover, (5.28) with $v = 0$ together with $s^* \geq \lambda^{-1/\gamma}$ implies

$$\mathcal{Q}_{D_m,\lambda} \leq (\tilde{c}^2 + \tilde{c} + 1).$$

Furthermore, (5.27) and (5.25) with $v = 0$ yield that with confidence at least $1 - \delta$, there holds

$$\mathcal{Q}_{D,\lambda} \mathcal{P}_{D,\lambda} \leq \tilde{c}'(\tilde{c}^2 + \tilde{c} + 1) \lambda^{-\frac{d}{4\gamma}} |D|^{-1/2} \log \frac{3}{\delta}.$$

Plugging the above three estimates into Proposition 5.10, we know

$$\begin{aligned} \|f_{D,s^*,\lambda} - f^*\|_{\psi} &\leq (1 + \tilde{c}(\tilde{c}^2 + \tilde{c} + 1))(1 + (\tilde{c}^2 + \tilde{c} + 1)^{\frac{\alpha-\beta}{2}}) \|f^*\|_{\varphi} \lambda^{\frac{\alpha-\beta}{2}} \\ &+ \tilde{c}'(\tilde{c}^2 + \tilde{c} + 1) \lambda^{-\frac{d}{4\gamma}} |D|^{-1/2} \log \frac{3}{\delta} \end{aligned}$$

holds with confidence $1 - \delta$. Noting further $\lambda = \bar{c} |D|^{-\frac{2\gamma}{2\gamma(\alpha-\beta)+d}}$ for some absolute constant $\bar{c} > 0$, we have

$$\|f_{D,s^*,\lambda} - f^*\|_{\psi} \leq C |D|^{-\frac{\gamma(\alpha-\beta)}{2\gamma(\alpha-\beta)+d}} \log \frac{3}{\delta},$$

where

$$C := (1 + \tilde{c}(\tilde{c}^2 + \tilde{c} + 1))(\bar{c} + \bar{c}(\tilde{c}^2 + \tilde{c} + 1)^{\frac{\alpha-\beta}{2}}) \|h^*\|_{\psi} + \tilde{c}'(\tilde{c}^2 + \tilde{c} + 1).$$

The only thing left is to present the range of s^* . Since $s^* \geq \lambda^{-1/\gamma}$ and $\lambda = \bar{c} |D|^{-\frac{2\gamma}{2\gamma(\alpha-\beta)+d}}$, we have

$$s^* \geq (\bar{c})^{-1/\gamma} |D|^{\frac{2}{2\gamma(\alpha-\beta)+d}}.$$

This completes the proof of Theorem 3.1. \square

5.6. Construction of hard-to-approximate target functions for lower bounds. To derive the lower bound, a crucial procedure is to construct hard-to-approximate target functions in \mathcal{N}_φ that cannot be approximated well. Denote $d_n^* = \sum_{k=n+1}^{2n} Z(d, k)$. Given $\tau > 0$, define a spherical polynomial by

$$(5.29) \quad f_{\omega, \tau, n} := \left(\frac{\tau}{d_n^*} \right)^{1/2} \sum_{k=n+1}^{2n} \hat{\phi}_k^{\beta/2} \sum_{\ell=1}^{Z(d, k)} \omega_{k, j} Y_{k, \ell},$$

where $\omega = (\omega_{n+1, 1}, \omega_{n+1, 2}, \dots, \omega_{2n, Z(d, 2n)}) \in \{0, 1\}^{d_n^*}$ is a binary string of size d_n^* . Then, for any n satisfying

$$(5.30) \quad (2\hat{c})^{\alpha-\beta} \tau n^{2\gamma(\alpha-\beta)} \leq U^2,$$

$\hat{c}^{-1} k^{-2\gamma} \leq \hat{\phi}_k \leq \hat{c} k^{-2\gamma}$ together with (3.2) yields

$$\begin{aligned} \|f_{\varepsilon, \tau, n}\|_\varphi^2 &\leq \frac{\tau}{d_n^*} \sum_{k=n+1}^{2n} Z(d, k) \hat{\phi}_k^{\beta-\alpha} \\ &\leq \frac{\tau}{d_n^*} \sum_{k=n+1}^{2n} Z(d, k) \hat{c}^{\alpha-\beta} k^{-2\gamma(\beta-\alpha)} \leq (2\hat{c})^{\alpha-\beta} \tau n^{2\gamma(\alpha-\beta)} \leq U^2. \end{aligned}$$

This implies $f_{\omega, \tau, n} \in \mathcal{N}_\varphi$ and $\|f_{\omega, \tau, n}\|_\varphi \leq U$. For another string $\omega' = (\omega'_{n+1, 1}, \dots, \omega'_{2n, Z(d, 2n)}) \in \{0, 1\}^{d_n^*}$, (3.2) and (3.1) also yield

$$(5.31) \quad \|f_{\omega, \tau, n} - f_{\omega', \tau, n}\|_{L^2(\mathbb{S}^d)}^2 = \frac{\tau}{d_n^*} \sum_{k=n+1}^{2n} \hat{\phi}_k^\beta \sum_{\ell=1}^{Z(d, k)} (\omega_{k, \ell} - \omega'_{k, \ell})^2 \leq \tau \hat{c}^\beta n^{-2\gamma\beta}.$$

We then aim to derive lower bound of $\|f_{\omega, \tau, n} - f_{\omega', \tau, n}\|_\psi$, for which the following Gilbert-Varahamov bound provided in [49, Lemma 2.9] (see also [18, Lemma 24]) is needed.

LEMMA 5.15. *For $S \geq 8$, there exist some $L \geq 2^{S/8}$ and some binary strings $\omega^{(0)}, \omega^{(1)}, \dots, \omega^{(L)} \in \{0, 1\}^S$ such that $\omega^{(0)} = 0$ and*

$$\sum_{j=1}^S (\omega_j^{(i)} - \omega_j^{(i')})^2 \geq S/8$$

for all $i \neq i'$, where $\omega^{(i)} = (\omega_1^{(i)}, \dots, \omega_S^{(i)})$.

If $S := d_n^* \geq 8$, let

$$(5.32) \quad \mathcal{E}_{n, L} := \{\omega^{*, i}\}_{i=1}^L$$

be the set of binary strings satisfying the conditions of Lemma 5.15. Then it follows from Lemma 5.15 that for any $\omega^{*, i}, \omega^{*, i'} \in \mathcal{E}_{n, L}$, there holds

$$(5.33) \quad \|f_{\omega^{*, i}, \tau, n} - f_{\omega^{*, i'}, \tau, n}\|_\psi^2 = \frac{\tau}{d_n^*} \sum_{k=n+1}^{2n} \sum_{\ell=1}^{Z(d, k)} (\omega_{k, \ell} - \omega'_{k, \ell})^2 \geq \tau/8.$$

5.7. Proof of Theorem 3.2. Set $f^* = f_{\omega^{*(\iota)}, \tau, n}$ for some τ and n satisfying (5.30) and $\omega^{*(\iota)} \in \mathcal{E}_{n, L}$ with $1 \leq \iota \leq L$. Let the noise $\{\varepsilon_i\}$ be drawn i.i.d. from the normal distribution $\mathcal{N}(0, M^2)$. We obtain a probability measure

$$\rho_{\omega^{*(\iota)}, \tau, n} = \rho_{\mathcal{T}_t}(dx) \times \mathcal{N}(f_{\omega^{*(\iota)}, \tau, n}, M^2),$$

where $\mathcal{T}_t = \{x_i\}_{i=1}^{|D|}$ is the spherical t -design and $\rho_{\mathcal{T}_s}(dx)$ denotes the deterministic and discrete distribution on the sphere satisfying

$$\int_{\mathbb{S}^d} f(x) \rho_{\mathcal{T}_s}(dx) = \frac{1}{|D|} \sum_{x_i \in \mathcal{T}_t} f(x_i).$$

It is easy to check that the data D generated by $\rho_{\omega^{*(\iota)}, \tau, n}$ satisfies (1.1).

For any f_D derived from D , define

$$(5.34) \quad \Phi(D) := \arg \min_{\iota=0, 1, \dots, L} \|f_D - f_{\omega^{*(\iota)}, \tau, n}\|_{\beta}.$$

Then for any $\iota \in \{0, \dots, L\}$ with $\iota \neq \Phi(D)$, we have from (5.33) that

$$(5.35) \quad \begin{aligned} \sqrt{\tau/8} &\leq \|f_{\omega^{*(\Phi(D)), \tau, n} - f_{\omega^{*(\iota)}, \tau, n}\|_{\psi} \\ &\leq \|f_{\omega^{*(\Phi(D)), \tau, n} - f_D\|_{\psi} + \|f_D - f_{\omega^{*(\iota)}, \tau, n}\|_{\psi} \leq 2\|f_D - f_{\omega^{*(\iota)}, \tau, n}\|_{\psi}. \end{aligned}$$

Therefore,

$$(5.36) \quad \mathbf{P}_{\rho_{\omega^{*(\iota)}, \tau, n}^{|D|}} [D : \|f_D - f_{\omega^{*(\iota)}, \tau, n}\|_{\psi}^2 \geq \tau/32] \geq \mathbf{P}_{\rho_{\omega^{*(\iota)}, \tau, n}^{|D|}} [D : \Phi(D) \neq \iota],$$

where $\rho^{|D|} = \overbrace{\rho \times \dots \times \rho}^{|D|}$ and $\iota = 0, 1, \dots, L$.

DEFINITION 5.16. Let ρ_1 and ρ_2 be two probability measures on some common measurable space (Ω, \mathcal{A}) satisfying that ρ_1 is absolutely continuous with respect to ρ_2 , then the Kullback-Leibler divergence for probability measures ρ_1 and ρ_2 is defined as

$$\mathcal{K}(\rho_1, \rho_2) := \int_{\Omega} \log \left(\frac{d\rho_1}{d\rho_2} \right) d\rho_1.$$

To lower bound $\mathbf{P}_{\rho_{\omega^{*(\iota)}, \tau, n}^{|D|}} [D : \Phi(D) \neq \iota]$, we recall the following lemma derived in [18, Lemma 20].

LEMMA 5.17. Let $L \geq 2$ and (Ω, \mathcal{A}) be a measurable space. Let $0 < c_* < \infty$, $\rho_0, \rho_1, \dots, \rho_L$ be probability measures on (Ω, \mathcal{A}) , and ρ_i be absolutely continuous with respect to ρ_0 for $i = 1, 2, \dots, L$ satisfying

$$\frac{1}{L} \sum_{i=1}^L \mathcal{K}(\rho_i, \rho_0) \leq c_*.$$

Then for all measurable functions $\Phi : \Omega \rightarrow \{0, 1, \dots, L\}$, there holds

$$\max_{i=0, 1, \dots, L} \mathbf{P}_{\rho_i} [D \in \Omega : \Phi(D) \neq i] \geq \frac{\sqrt{L}}{1 + \sqrt{L}} \left(1 - \frac{3c_*}{\log L} - \frac{1}{2 \log L} \right).$$

Based on the above foundations, we can prove Theorem 3.2 as follows.

Proof of Theorem 3.2. Let $\rho_1 = \rho_{\omega^{*(t)}, \tau, n}$ and $\rho_2 = \rho_{\omega^{*(0)}, \tau, n}$ be the same as in Lemma 5.17. Due to the definition of the Kullback-Leibler divergence, it is easy to derive [5, P.998]

$$\mathcal{K}(\rho_1^{D|}, \rho_2^{D|}) = |D|\mathcal{K}(\rho_1, \rho_2),$$

and

$$\mathcal{K}(\mathcal{N}(f_{\omega^{*(t)}, \tau, n}, M^2), \mathcal{N}(f_{\omega^{*(0)}, \tau, n}, M^2)) = \frac{(f_{\omega^{*(t)}, \tau, n} - f_{\omega^{*(0)}, \tau, n})^2}{2M^2}.$$

Since $f_{\omega, \tau, n}$ defined by (5.29) is a spherical polynomial of degree at most $2n$, then for

$$(5.37) \quad n \leq t/2,$$

we have from (5.31) and the definition of the spherical t -design that

$$\begin{aligned} \frac{1}{L} \sum_{i=1}^L \mathcal{K}(\rho_{\omega^{*(t)}, \tau, n}^{D|}, \rho_{\omega^{*(0)}, \tau, n}^{D|}) &= \frac{|D|}{M^2} \frac{1}{L} \sum_{i=1}^L \frac{1}{|D|} \sum_{i=1}^{|D|} (f_{\omega^{*(t)}, \tau, n}(x_i) - f_{\omega^{*(0)}, \tau, n}(x_i))^2 \\ &= \frac{|D|}{M^2} \frac{1}{L} \sum_{i=1}^L \|f_{\omega^{*(t)}, \tau, n} - f_{\omega^{*(0)}, \tau, n}\|_{L^2(\mathbb{S}^d)}^2 \leq \frac{\hat{c}^\beta |D| \tau}{M^2 n^{2\gamma\beta}} =: c_*. \end{aligned}$$

Setting $\mathcal{D} = D$ in Lemma 5.17, we get

$$\max_{i=0,1,\dots,L} \mathbf{P}_{\rho_{\omega^{*(i)}, \tau, n}} [D : \Phi(D) \neq i] \geq \frac{\sqrt{L}}{1 + \sqrt{L}} \left(1 - \frac{3\hat{c}^\beta |D| \tau}{M^2 n^{2\gamma\beta} \log L} - \frac{1}{2 \log L} \right),$$

where $L \geq 2^{d_n^*}/8$. This together with (5.36) and $d_n^* \leq Z(d+1, 2n) \leq 2^d n^d$ yields that there is a probability distribution ρ^* and a function f_{bad}^* satisfying (1.1) such that

$$\mathbf{P}_{\rho^*} [D : \|f_D - f_{bad}^*\|_\psi^2 \geq \tau/32] \geq \frac{1}{2} \left(1 - \frac{12\hat{c}^\beta |D| \tau}{2^d M^2 n^{2\gamma\beta+d}} - \frac{4}{2^d n^d} \right).$$

The only thing left is to select suitable τ and n to satisfy (5.30) and (5.37).

Since $\hat{c}_1^{-1} |D|^{1/d} \leq s \leq \hat{c}_1 |D|^{1/d}$ for some $\hat{c}_1 \geq 1$, if $\tau = C_1'' |D|^{-\frac{2\gamma(\alpha-\beta)}{2\gamma(\alpha-\beta)+d}}$ and $n = C_1' |D|^{\frac{1}{2\gamma(\alpha-\beta)+d}}$ with $C_1' = \min \left\{ \frac{2}{\gamma(\alpha-\beta)} (2\hat{c})^{-\frac{1}{\gamma}} (U^2 C_1'')^{-\frac{1}{\gamma(\alpha-\beta)}}, \frac{\hat{c}_1}{2} \right\}$ and C_1'' small enough such that

$$\max \left\{ \frac{12\hat{c}^\beta C_1''}{2^d M^2 (C_1')^{2\gamma\beta+d}}, \frac{4}{2^d (C_1')^d} \right\} \leq \frac{1}{4},$$

then (5.30) and (5.37) hold, and

$$\mathbf{P}_{\rho^*} [D : \|f_D - f_{bad}^*\|_\psi \geq C_1 |D|^{-\frac{\gamma(\alpha-\beta)}{2\gamma(\alpha-\beta)+d}}] \geq \frac{1}{2} \left(1 - \frac{1}{2} |D|^{-\frac{\min\{2\gamma\beta, d\}}{2\gamma(\alpha-\beta)+d}} \right) \geq \frac{1}{4},$$

where $C_1 = (C_1''/32)^{1/2}$. This completes the proof of Theorem 3.2. \square

REFERENCES

- [1] C. AN, X. CHEN, I. H. SLOAN, AND R. S. WOMERSLEY, *Regularized least squares approximations on the sphere using spherical designs*, SIAM Journal on Numerical Analysis, 50 (2012), pp. 1513–1534.
- [2] C. AN AND H.-N. WU, *Lasso hyperinterpolation over general regions*, SIAM Journal on Scientific Computing, 43 (2021), pp. A3967–A3991.

- [3] E. BANNAI AND E. BANNAI, *A survey on spherical designs and algebraic combinatorics on spheres*, European Journal of Combinatorics, 30 (2009), pp. 1392–1425.
- [4] R. BHATIA, *Matrix Analysis*, vol. 169, Springer Science & Business Media, 2013.
- [5] G. BLANCHARD AND N. MÜCKE, *Optimal rates for regularization of statistical inverse learning problems*, Foundations of Computational Mathematics, 18 (2018), pp. 971–1013.
- [6] A. BONDARENKO, D. RADCHENKO, AND M. VIAZOVSKA, *Optimal asymptotic bounds for spherical designs*, Annals of Mathematics, (2013), pp. 443–452.
- [7] A. BONDARENKO, D. RADCHENKO, AND M. VIAZOVSKA, *Well-separated spherical designs*, Constructive Approximation, 41 (2015), pp. 93–112.
- [8] J. S. BRAUCHART AND P. J. GRABNER, *Distributing many points on spheres: minimal energy and designs*, Journal of Complexity, 31 (2015), pp. 293–326.
- [9] J. S. BRAUCHART AND K. HESSE, *Numerical integration over spheres of arbitrary dimension*, Constructive Approximation, 25 (2007), pp. 41–71.
- [10] G. BROWN AND F. DAI, *Approximation of smooth functions on compact two-point homogeneous spaces*, Journal of Functional Analysis, 220 (2005), pp. 401–423.
- [11] X. CHEN AND R. S. WOMERSLEY, *Existence of solutions to systems of underdetermined equations and spherical designs*, SIAM Journal on Numerical Analysis, 44 (2006), pp. 2326–2341.
- [12] X. CHEN AND R. S. WOMERSLEY, *Spherical designs and nonconvex minimization for recovery of sparse signals on the sphere*, SIAM Journal on Imaging Sciences, 11 (2018), pp. 1390–1415.
- [13] A. CHERNIH, I. H. SLOAN, AND R. S. WOMERSLEY, *Wendland functions with increasing smoothness converge to a Gaussian*, Advances in Computational Mathematics, 40 (2014), pp. 185–200.
- [14] C. H. CHOI, J. IVANIC, M. S. GORDON, AND K. RUEDENBERG, *Rapid and stable determination of rotation matrices between spherical harmonics by direct recursion*, Journal of Chemical Physics, 111 (1999), pp. 8825–8831.
- [15] P. DELSARTE, J. M. GOETHALS, AND J. J. SEIDEL, *Spherical codes and designs*, Geometriae Dedicata, 6 (1977), pp. 363–388.
- [16] H. W. ENGL, M. HANKE, AND A. NEUBAUER, *Regularization of Inverse Problems*, vol. 375, Springer Science & Business Media, 1996.
- [17] H. FENG, S.-B. LIN, AND D.-X. ZHOU, *Radial basis function approximation with distributively stored data on spheres*, arXiv:2112.02499, (2021).
- [18] S. FISCHER AND I. STEINWART, *Sobolev norm learning rates for regularized least-squares algorithms.*, Journal of Machine Learning Research, 21 (2020), pp. 1–38.
- [19] W. GAO, X. SUN, Z. WU, AND X. ZHOU, *Multivariate Monte Carlo approximation based on scattered data*, SIAM Journal on Scientific Computing, 42 (2020), pp. A2262–A2280.
- [20] M. GRÄF AND D. POTTS, *On the computation of spherical designs by a new optimization approach based on fast spherical fourier transforms*, Numerische Mathematik, 119 (2011), pp. 699–724.
- [21] L. GYÖRFI, M. KOHLER, A. KRZYŻAK, AND H. WALK, *A Distribution-free Theory of Nonparametric Regression*, vol. 1, Springer, 2002.
- [22] T. HANGELBROEK, F. J. NARCOWICH, X. SUN, AND J. D. WARD, *Kernel approximation on manifolds ii: The l_∞ norm of the l_2 projector*, SIAM Journal on Mathematical Analysis, 43 (2011), pp. 662–684.
- [23] T. HANGELBROEK, F. J. NARCOWICH, AND J. D. WARD, *Kernel approximation on manifolds i: bounding the Lebesgue constant*, SIAM Journal on Mathematical Analysis, 42 (2010), pp. 1732–1760.
- [24] R. HARDIN AND N. SLOANE, *A new approach to the construction of optimal designs*, Journal of Statistical Planning and Inference, 37 (1993), pp. 339–369.
- [25] K. HESSE, I. H. SLOAN, AND R. S. WOMERSLEY, *Radial basis function approximation of noisy scattered data on the sphere*, Numerische Mathematik, 137 (2017), pp. 579–605.
- [26] N. JAROSIK, C. BENNETT, J. DUNKLEY, B. GOLD, M. GREASON, M. HALPERN, R. HILL, G. HINSHAW, A. KOGUT, E. KOMATSU, ET AL., *Seven-year wilkinson microwave anisotropy probe (wmap*) observations: sky maps, systematic errors, and basic results*, Astrophysical Journal Supplement Series, 192 (2011), pp. 1–15.
- [27] M. A. KING, R. J. BINGHAM, P. MOORE, P. L. WHITEHOUSE, M. J. BENTLEY, AND G. A. MILNE, *Lower satellite-gravimetry estimates of antarctic sea-level contribution*, Nature, 491 (2012), pp. 586–589.
- [28] Q. T. LE GIA AND H. MHASKAR, *Localized linear polynomial operators and quadrature formulas on the sphere*, SIAM Journal on Numerical Analysis, (2008), pp. 440–466.
- [29] Q. T. LE GIA, F. J. NARCOWICH, J. D. WARD, AND H. WENDLAND, *Continuous and discrete least-squares approximation by radial basis functions on spheres*, Journal of Approximation

- Theory, 143 (2006), pp. 124–133.
- [30] Q. T. LE GIA, I. H. SLOAN, AND H. WENDLAND, *Multiscale analysis in sobolev spaces on the sphere*, SIAM journal on numerical analysis, 48 (2010), pp. 2065–2090.
 - [31] P. LEOPARDI, *A partition of the unit sphere into regions of equal area and small diameter*, Electronic Transactions on Numerical Analysis, 25 (2006), pp. 309–327.
 - [32] J. LEVESLEY AND X. SUN, *Approximation in rough native spaces by shifts of smooth kernels on spheres*, Journal of Approximation Theory, 133 (2005), pp. 269–283.
 - [33] S.-B. LIN, X. GUO, AND D.-X. ZHOU, *Distributed learning with regularized least squares*, Journal of Machine Learning Research, 18 (2017), pp. 3202–3232.
 - [34] S.-B. LIN, Y. G. WANG, AND D.-X. ZHOU, *Distributed filtered hyperinterpolation for noisy data on the sphere*, SIAM Journal on Numerical Analysis, 59 (2021), pp. 634–659.
 - [35] S. LU, P. MATHÉ, AND S. PEREVERZYEV JR, *Analysis of regularized Nyström subsampling for regression functions of low smoothness*, Analysis and Applications, 17 (2019), pp. 931–946.
 - [36] J. D. MCEWEN, G. PUY, J.-P. THIRAN, P. VANDERGHEYNST, D. VAN DE VILLE, AND Y. WIAUX, *Sparse image reconstruction on the sphere: implications of a new sampling theorem*, IEEE Transactions on Image Processing, 22 (2013), pp. 2275–2285.
 - [37] J. D. MCEWEN AND Y. WIAUX, *A novel sampling theorem on the sphere*, IEEE Transactions on Signal Processing, 59 (2011), pp. 5876–5887.
 - [38] H. MHASKAR, F. NARCOWICH, AND J. WARD, *Spherical marcinkiewicz-zygmund inequalities and positive quadrature*, Mathematics of Computation, 70 (2001), pp. 1113–1130.
 - [39] C. MÜLLER, *Spherical Harmonics*, vol. 17, Springer, 1966.
 - [40] F. J. NARCOWICH, N. SIVAKUMAR, AND J. D. WARD, *Stability results for scattered-data interpolation on euclidean spheres*, Advances in Computational Mathematics, 8 (1998), pp. 137–163.
 - [41] F. J. NARCOWICH, X. SUN, J. D. WARD, AND H. WENDLAND, *Direct and inverse sobolev error estimates for scattered data interpolation via spherical basis functions*, Foundations of Computational Mathematics, 7 (2007), pp. 369–390.
 - [42] F. J. NARCOWICH AND J. D. WARD, *Scattered data interpolation on spheres: error estimates and locally supported basis functions*, SIAM Journal on Mathematical Analysis, 33 (2002), pp. 1393–1410.
 - [43] R. J. RENKA, *Multivariate interpolation of large sets of scattered data*, ACM Transactions on Mathematical Software (TOMS), 14 (1988), pp. 139–148.
 - [44] A. RUDI, R. CAMORIANO, AND L. ROSASCO, *Less is more: Nyström computational regularization*, in NIPS, 2015, pp. 1657–1665.
 - [45] S. SMALE AND D.-X. ZHOU, *Shannon sampling and function reconstruction from point values*, Bulletin of the American Mathematical Society, 41 (2004), pp. 279–305.
 - [46] S. SMALE AND D.-X. ZHOU, *Shannon sampling II: Connections to learning theory*, Applied and Computational Harmonic Analysis, 19 (2005), pp. 285–302.
 - [47] Z. SUN, M. DAI, Y. WANG, AND S.-B. LIN, *Nyström regularization for time series forecasting*, arXiv preprint arXiv:2111.07109, (2021).
 - [48] Y.-T. TSAI AND Z.-C. SHIH, *All-frequency precomputed radiance transfer using spherical radial basis functions and clustered tensor approximation*, ACM Transactions on Graphics (TOG), 25 (2006), pp. 967–976.
 - [49] A. B. TSYBAKOV, *Introduction to Nonparametric Estimation*, Springer, 2009.
 - [50] G. WAHBA, *Spline interpolation and smoothing on the sphere*, SIAM Journal on Scientific and Statistical Computing, 2 (1981), pp. 5–16.
 - [51] M. A. WIECZOREK AND R. J. PHILLIPS, *Potential anomalies on a sphere: Applications to the thickness of the lunar crust*, Journal of Geophysical Research: Planets, 103 (1998), pp. 1715–1724.
 - [52] R. S. WOMERSLEY, *Efficient spherical designs with good geometric properties*, in Contemporary computational mathematics—A celebration of the 80th birthday of Ian Sloan, Springer, 2018, pp. 1243–1285.
 - [53] R. S. WOMERSLEY AND I. H. SLOAN, *How good can polynomial interpolation on the sphere be?*, Advances in Computational Mathematics, 14 (2001), pp. 195–226.
 - [54] V. A. YUDIN, *Coverings of a sphere, and extremal properties of orthogonal polynomials*, Diskretnaya Matematika, 7 (1995), pp. 81–88.
 - [55] Y. ZHANG, J. DUCHI, AND M. WAINWRIGHT, *Divide and conquer kernel ridge regression: A distributed algorithm with minimax optimal rates*, Journal of Machine Learning Research, 16 (2015), pp. 3299–3340.
 - [56] D.-X. ZHOU, *Deep distributed convolutional neural networks: Universality*, Analysis and Applications, 16 (2018), pp. 895–919.